Initial Dilution of a Horizontal Jet in a Strong Current

by

Bonnie Jean Marks

B.A.Sc., The University of Waterloo, 1994

A THESIS SUBMITTED IN PARTIAL FULFILLMENT OF

THE REQUIREMENTS FOR THE DEGREE OF

MASTER OF APPLIED SCIENCE

in

THE FACULTY OF GRADUATE STUDIES

Department of Civil Engineering

We accept this thesis as conforming to the required standard

THE UNIVERSITY OF BRITISH COLUMBIA

August 1996

©Bonnie Jean Marks, 1996

In presenting this thesis in partial fulfilment of the requirements for an advanced degree at the University of British Columbia, I agree that the Library shall make it freely available for reference and study. I further agree that permission for extensive copying of this thesis for scholarly purposes may be granted by the head of my department or by his or her representatives. It is understood that copying or publication of this thesis for financial gain shall not be allowed without my written permission.

Department of Civil Engineering
The University of British Columbia
Vancouver, Canada

August 21, 1996

ABSTRACT

The initial dilution of waste discharging into a water body can be accomplished by turbulent jets. Enhanced mixing is thought to occur when the water body is a river, due to the presence of an ambient current and increased turbulence levels. One case of jet mixing in a river is when the jet is weak compared with the ambient current, such as a pulp mill discharge into the Fraser River.

This research was initially driven by the need to model the interaction between suspended sediments and pulp mill effluent in the Fraser River Basin under the Fraser River Action Plan. Because of the detrimental effect on water quality, researchers are investigating the physical, chemical and biological processes which occur when an effluent plume is discharged into the river. This study examines the physical mechanisms which are responsible for mixing in the vicinity of the discharge.

To investigate the mixing process in the initial near-field, experiments involving a single buoyant jet discharging at an angle of 45 degrees into a moving ambient environment were performed. The main emphasis of this study is on using temperature measurements to calculate dilution in the vicinity of the port. To simulate field conditions in the laboratory, the range of two modelling parameters were preserved, namely the densimetric jet Froude number and the velocity ratio, which is the ratio of jet velocity to ambient velocity.

The experimental data showed that the velocity ratio has a greater influence on dilution than the jet Froude number. Generally, dilution increases with decreasing velocity ratio or increasing ambient current. The data correspond well with previous studies on dilution of jet in a perpendicular crossflow. Bottom attachment of the jet is evident, creating a possible mechanism for entrainment of bottom sediments into the effluent plume in relation to the Fraser River.

TABLE OF CONTENTS

ABSTRACT ii

TABLE OF CONTENTS iii

LIST OF TABLES v

LIST OF FIGURES vi

LIST OF SYMBOLS viii

ACKNOWLEDGMENTS ix

1.0 INTRODUCTION 1

1.1 Mixing Zones and Governing Parameters 2

1.2 Study Scope and Objective 3

1.3 Ambient Environment - Fraser River 6

1.4 Diffuser Characteristics and Effluent Parameters - Northwood 6

2.0 LITERATURE REVIEW 13

2.1 Buoyant Jets 13
2.1.1 Initial Zone of Flow Establishment 16

2.2 Length Scales 17

2.3 Previous Experimental Research 19
2.3.1 Boundary Interactions 19
2.3.2 Ambient Current 21
2.3.3 Port Orientation 22

2.4 Modelling of Near-field Mixing 27
2.4.1 Introduction to CORMIX 1 28

3.0 LABORATORY EXPERIMENTS 35

3.1 Experimental Design 37

3.2 Physical Set-up 38

3.3 Experimental Procedure 39

3.4 Ambient Characterization 40

4.0 RESULTS, ANALYSIS AND DISCUSSION OF DATA 44

4.1 Dilution 45
4.1.1 Dilution for Varying Froude Number and Velocity Ratio 46
4.1.2 Non-Dimensional Dilution 47
4.1.3 Comparison with CORMIX 1 Output 49

4.2 Temperature Contour Plots 51

4.3 Jet Centerline Trajectory 52

4.4 Concentration Profiles 53

4.5 Temperature-Time Series 54

5.0 CONCLUSIONS AND RECOMMENDATIONS 71

5.1 Summary of Experiment Results 71

5.2 Main Conclusions 72

5.3 Applicability to Northwood and the Fraser River 73

5.4 Recommendations 74

6.0 REFERENCES 75

APPENDIX A: THERMOCOUPLE CALIBRATION INFORMATION 78

LIST OF TABLES

Table 2. 1: Description of Flow Behaviour Regime and Length Scale Range **23**

Table 2. 2: Summary of Dilution Coefficient α from Previous Research **27**

Table 3. 1: Monthly Values of R Based on the Northwood Port Velocity, U_j and Fraser River Velocity, U_a **36**

Table 3. 2: Seasonal Changes in Parameters at Northwood Based on Field Data and Environment Canada Data **36**

Table 3. 3: Details for Each Experiment **37**

Table 4. 1: Length Scales for Experiments 1 to 12 ..... **45**

Table 4. 2: Values of Coefficient α for Experiments 1 to 12 ..... **48**

Table A. 1: Calibration Slope and Offset Values for Individual Thermocouples **79**

LIST OF FIGURES

Figure 1. 1: Plan and profile schematics of the near- and far-field mixing zones showing the controlling mixing mechanisms in each zone. **8**

Figure 1. 2: Detailed schematic of the near-field mixing zone describing important parameters and interactions. **9**

Figure 1. 3: Hydrograph for the Fraser River at the Environment Canada station at Shelly, 20 km upstream of Prince George **10**

Figure 1. 4: Plan view of the Northwood multiport diffuser structure. Diffuser is oriented perpendicular to the Fraser River and individual ports discharge effluent at 45° to the flow **11**

Figure 1. 5: Plot of the average daily effluent flow rate at Northwood for a three year period, data provided by Environment Canada. The solid line is the average monthly effluent flow rate of 1.7 m^3/s **12**

Figure 2. 1: The initial jet discharge zone encompasses the zone of flow establishment, ZFE, and the zone of established flow, ZEF **31**

Figure 2. 2: Length scale schematics: (a) jet to plume length scale, (b) jet to crossflow length scale, (c) plume to crossflow length scale. **32**

Figure 2. 3: Coanda attachment is caused by the pressure distribution and entrainment demand of the jet (Wood, 1994). Higher velocities exist below the jet and the lower pressure by Bernoulli's' effects cause the jet's centerline to move towards the boundary. **33**

Figure 2. 4: Flow classification chart for CORMIX 1 mixing model (Jirka and Doneker, 1991). Chart is for horizontal or vertical discharges in an uniform density ambient environment. **34**

Figure 3. 1: Plan and profile schematics of the general experimental set-up describing the important parameters and dimensions. **41**

Figure 3. 2: Details of the experimental configuration (a) Schematic (b) Photograph **42**

Figure 3. 3: Ambient velocity characterization of the laboratory flume to show port is discharging into the top of boundary layer. **43**

Figure 4. 1: Dilution with downstream distance (a) for varying Froude number but similar velocity ratio (R=1) and (b) for varying velocity ratio but similar Froude number (Fr=8). The Froude number has minimal influence on the initial dilution, since jet flow behaviour is moment-dominated. Minimum dilution increases with decreasing velocity ratio as expected. **56**

Figure 4. 2: (a) Plot of S_{min} versus x/L_m for the limits of velocity ratio, showing data points within the MDFF length scale range, $x>L_m$ and $x<L_M$, correlate to the 2/3 power. (b) Similar plot for all experiments showing that dilution is dependent on R. **57**

Figure 4. 3: Variation of experimental coefficient, α, with velocity ratio, R. The coefficient increases with decreasing R. **58**

Figure 4. 4: Plots of velocity ratio versus changes in ambient Reynolds number, ambient velocity and jet Froude number along with respective coefficient value. **59**

Figure 4. 5: Comparison of experimental dilution data with CORMIX 1 output for $R > 1$. **60**

Figure 4. 6: Comparison of experimental dilution data with CORMIX 1 output for $R \leq 1$. **61**

Figure 4. 7: Contour plot of excess temperature, defined as the temperature above ambient, for experiment #7. Each frame shows the jet at a farther downstream station **62**

Figure 4. 8: Contour plots of excess temperature, defined as the temperature above ambient, for experiment #9. Each frame shows the jet at a farther downstream location. **63**

Figure 4. 9: Jet trajectory in the y-x plane for experiments 1 to 8. Jet is quickly advected by the ambient current and the penetration distance reduces with decreasing R. **64**

Figure 4. 10: Jet trajectory in the x-z plane for experiments 1 to 8 and experiments 9 to 12. Jet centerline is attracted towards the bed due to possible Coanda attachment of jet. **65**

Figure 4. 11: Depth average horizontal concentration profiles for experiments #3 and 12. The jet horizontal width increases with distance and decreasing ambient velocity. **66**

Figure 4. 12: Vertical concentration profiles with distance for experiments #3 and 12. Profiles show vertical jet width increases with distance and decreasing ambient velocity. Higher velocities promote attachment of the jet to the flume bottom. **67**

Figure 4. 13: Plot of maximum turbulence intensity with distance away from source. Turbulence intensity is on order of 0.1. ..... **68**

Figure 4. 14: Depth averaged horizontal turbulence intensity profiles for experiment #3. The width of the turbulent zone increases and peak values decrease with distance. **69**

Figure 4. 15: Depth averaged horizontal turbulence intensity profiles for experiment #12. Peak values are slightly higher on the side where the current initially impacts the jet. **70**

Figure A. 1: Calibration curves for individual thermocouples **80**

LIST OF SYMBOLS

A	cross-sectional area of jet
B	buoyancy flux
b_T	Gaussian concentration half-width
b_w	Gaussian axial velocity half-width
C	concentration
C_2	experimental trajectory coefficient
C_6	experimental dilution coefficient
d	port diameter
Fr	densimetric jet Froude number
g	gravitational acceleration
g_o'	reduced gravitational constant
h_o	height of water above port
L_b	plume to crossflow length scale
L_M	jet to plume length scale
L_m	jet to crossflow length scale
L_Q	geometric length scale
M	momentum flux
Q	flow rate
R	ratio of jet velocity to ambient velocity
S	dilution
T	temperature
ΔT	temperature difference between jet and ambient
U	velocity
w	time-averaged axial jet velocity
x	horizontal distance parallel to current
y	horizontal distance perpendicular to current
z	vertical distance
Z_o	distance between bottom and port centerline
α	experimental coefficient
θ	port angle
ρ	density
$\Delta\rho$	density difference between jet and ambient
μ	specific mass flux

<u>Subscripts</u>

a	ambient
cl	centerline
j	jet
m	maximum
min	minimum
mean	average
o	initial

ACKNOWLEDGMENTS

I would like to thank the my supervisor, Dr. Greg Lawrence, for his intellectual and financial support, for taking me on when already overloaded with students and for the introduction into the fascinating world of environmental fluid mechanics. Thanks to Dr. Michael Quick for taking the time to read my thesis and supplying me with teaching assistantships. Thanks to Kurt Nielson from the Civil Engineering Hydraulics Lab for building parts of the experimental apparatus and Scott Jackson for developing the computer program. And special thanks to Jason Vine for the amazing amounts of help and support during my time at UBC, and for being my coffee buddy.

1.0 INTRODUCTION

Most of society's urban and industrial wastes are discharged into rivers, lakes, oceans or the atmosphere. These wastes become dilute as they mix with the surrounding fluid. Many of these discharges are in the form of a jet or plume, in which fluid from an orifice or slot flows into a large body of the same or similar fluid. Jets and plumes, especially if turbulent, are an effective method to accomplish mixing of effluent discharges, since they allow for the entrainment of large volumes of surrounding fluid and rapid initial dilution. Discharges are classified as buoyant jets when they have a source of momentum and buoyancy, where the buoyancy is caused by the density difference between discharge and the surrounding fluid.

To minimize the effect on the environment in the vicinity of the discharge, initial dilution of effluent can be enhanced by more complex structures involving turbulent jets and plumes. Jet mixing has been examined in detail for varying geometries and ambient fluid conditions (Fischer *et al.*, 1979 and Wood *et al.*, 1993). However, mixing of a turbulent jet discharging into a river has received relatively little attention.

When discharging into a river, the complexity of the problem is increased by introducing a flowing ambient environment. The ambient current transports the effluent away from the source, and the surrounding turbulence levels cause further dilution of the effluent in addition to the jet mixing mechanisms of momentum and buoyancy. When the ambient environment is a river, proximity to the boundaries and depth of water become important additional mixing parameters.

The present study examines the initial dilution of a horizontal turbulent jet, oriented at 45 degrees, discharging into a shallow moving environment. Since the ambient velocity is greater than the jet

velocity in the direction of the flow, this study represents an example of a weak jet in a strong current. A specific example of this problem is a pulp mill effluent discharge through a multiport diffuser into the Fraser River in British Columbia.

1.1 Mixing Zones and Governing Parameters

Mixing in rivers can be described in terms of the near-field and far-field mixing zones. The near-field is defined as the area between the discharge structure and the location where the effluent is vertically mixed in the river. It encompasses buoyant jet mixing and boundary interactions. Far-field mixing occurs after the effluent plume is vertically mixed, and encompasses transverse and longitudinal mixing in the river due to buoyant spreading and passive diffusion. A generalized schematic showing the mixing zones and controlling mixing mechanisms is provided in Figure 1.1.

Initial mixing in the near-field is caused by a turbulent shear layer that forms between the discharge and the ambient environment. The discharge or buoyant jet entrains ambient fluid and is diluted, increasing the width of the turbulent zone with distance from the discharge. The initial dilution is obtained by the entrainment of the surrounding ambient fluid, reducing contaminant concentrations and in relation to this study, bringing river sediment and effluent biosolids into contact. A near-field schematic is provided in Figure 1.2.

Near-field mixing is a complex process influenced by diffuser characteristics, effluent parameters and ambient conditions (Fischer *et al.*, 1979). In the near-field, mixing of effluent and ambient water is controlled by the buoyancy and momentum flux of the diffuser jets, their orientation, and the density and velocity structure of the ambient environment. The initial fluxes of buoyancy and momentum are important, since they control the movement of the plume. In general, momentum

controls the movement across and down the river, while buoyancy governs to the behaviour of the plume in the vertical direction.

The important diffuser characteristics are the port diameter and its closeness to boundaries, as well as its orientation to the ambient current and location in the river. The effluent parameters which affect mixing are the flow rate or port velocity and the temperature of the effluent. The temperature difference between the effluent and the ambient environment provides the density difference and hence, the buoyancy force. The ambient conditions of significance are the velocity, depth of water column, water temperature and turbulence structure in the river.

In the far-field, the jet trajectory and mixing are controlled by the ambient conditions through buoyant spreading and passive diffusion. Buoyant spreading arises from the density difference and causes the plume to move in the transverse direction as it travels with the ambient current. Far from the source, passive diffusion becomes the dominant mixing mechanism when existing turbulence in the ambient environment is strong compared to jet turbulence.

1.2 Study Scope and Objective

Study Scope

The Fraser River Action Plan (FRAP) was created in 1991 to save one of B.C.'s most valuable ecosystems, the Fraser River Basin. Anthropogenic activities such as: agriculture, forestry, mining, urban development, power generation, fisheries, recreation and tourism are affecting the environmental quality of the Fraser River Basin. Pulp and paper mills are a major pollution source detrimental to the Fraser River. These mills discharge a complex wastewater containing a variety of contaminants that are toxic to both aquatic species and wildlife. The most destructive contaminants

are dioxins and furans which are chlorinated organic compounds, highly toxic and insoluble. These contaminants have been identified in water, sediment, fish and wildlife samples downstream from the pulp mills in the Fraser River Basin (Marmorek *et al.*, 1992).

To improve water quality and management of the Fraser River ecosystem, an understanding of the fate and transport of contaminants introduced into the river is needed. This involves characterizing the physical, chemical and biological processes involved in the near-field dispersion of contaminants away from the source. To assist in estimating contaminant transport by the interaction between these various processes, it is important to develop a hydrodynamic model which is capable of predicting pollutant concentrations downstream of effluent discharges. Ideally, such a model would include the effects of turbulent mixing and dispersion along with chemical reactions between contaminants or biosolids in the effluent with the suspended sediment in the river, specifically adsorption or flocculation.

This research is part of the investigation into the interaction between Fraser River suspended sediment and pulp mill effluent under FRAP. It is thought that pulp mill effluent promotes flocculation and enhances transport of contaminants in the river (Evans, 1996, Sekela *et al.*, 1995, Krishnappen *et al.*, 1994). Flocculation may be most dramatic in the first few metres from the discharge where dilution is low and turbulence levels are high. Because the effluent concentrations are elevated and important chemical reactions are occurring in this region, there is a need to examine the physical processes of jet mixing and dispersion of effluent near the discharge. Understanding jet mixing will provide a better spatial resolution of contaminant concentrations in the water column within the immediate area of discharge.

Study Objective

The interaction between pulp mill effluent and suspended sediment takes place in the area of initial contact between the discharge and the river. This initial zone is part of the near-field mixing zone. The near-field zone is very complex to model since seasonal changes exist in both the effluent and ambient parameters. As well, changes in ambient water depth, velocity and turbulence exist across and down the river. There are existing numerical models which predict initial dilution in the near-field region, however, modelling becomes more complex with different angle of discharge and the addition of an ambient current. Therefore, in order to understand and improve modelling capability in the near-field mixing zone experiments were conducted to investigate the controlling mechanisms or parameters on the initial dilution of effluent.

The experiments performed were based on conditions at a specific pulp mill, Northwood Pulp and Timber Ltd., and in the Fraser River. The primary objective was to investigate the effects of: seasonal changes in temperature and velocity, strong ambient current, shallow water depth, a 45° orientation of discharge on initial dilution, and other jet characteristics. A second objective was to relate important jet mixing parameters to the sediment and biosolids interaction (Evans, 1996) through dilution and turbulence intensity. Lastly, it was desired that concentration distributions in the river, at the end of the initial mixing zone, would be obtained to be used as input to another submodel for turbulent dispersion (Vine, 1996).

The last two objectives may serve to enhance the general Fraser River predictive model developed under FRAP by Gobas (1996). The model simulates the Fraser River as a series of completely mixed reactors. The purpose of this model is to predict the environmental and ecological fate of

organic chemical discharges in the water, sediments, benthic community and aquatic life in the Fraser River Basin, as a function of time and during different seasons of the year (Gobas, 1996).

1.3 Ambient Environment - Fraser River

The Fraser River drains approximately one quarter of British Columbia. The river discharge rises in April and May, peaks in June, and rapidly decreases in July as shown in Figure 1.3. After July, the flow slowly decreases to its winter base flow. There can be isolated peaks due to rainfall events during the year. The discharge rates can vary yearly depending on the snowpack. At the Environment Canada station at Shelly, 20 km upstream of Prince George, the average base flow is approximately 150 m^3/s and the springtime peak is $2400 m^3/s$.

The width, depth and velocity of the river varies seasonally along with the river temperature. The water depth in the vicinity of the diffuser varies between approximately 1 to 4 metres (Evans, 1996, Northwood, per comm.). Ambient water temperature ranges from 0 to 15 degrees Celsius. There is a high level of ambient turbulence in the river. The river transports sediment mainly in the spring months, and the suspended sediment concentrations follow the same trend as the discharge hydrograph (Sekela *et al.*, 1995).

1.4 Diffuser Characteristics and Effluent Parameters - Northwood

The first mill on the Fraser River is Northwood Pulp and Timber Ltd., located upstream of Prince George. Northwood's treatment system consists of clarifying tanks and biological treatment in aerated lagoons and a pre-discharge basin (Sekela *et al.*, 1995). The effluent is then discharged to the Fraser River through a submerged multiport diffuser. The contaminants of primary concern in

the pulp mill effluent are dioxins and furans. Field studies and air photos have shown three distinct plumes surfacing downstream of the diffuser (Evans, 1996, per.comm. and Borstad & Associates, per comm.).

The multiport diffuser consists of three risers with two ports per riser (Figure 1.4). The individual ports from the diffuser can be represented as distinct separate jets until they merge at some distance downstream. The diffuser is perpendicular to the flow and is approximately 30 metres in length from the first to last riser. The ports are 90 degrees apart and are oriented 45 degrees to the ambient flow. Each individual port has a diameter of 0.5 metres. The distance from the west bank of the river to the first riser is on order of 30 metres. The port centerline is approximately 0.3 meters from the river bottom according to the original design drawings completed in the 1960's, provided by Northwood.

The average daily effluent flow rates from 1992 to 1994 for Northwood, provided by Environment Canada, are plotted in Figure 1.5. The average flow rate into the diffuser is 1.7 m^3/s which corresponds to individual port velocities of 1.4 m/s. The minimum and maximum port discharge velocities are approximately 0.8 and 1.7 m/s, respectively, and there are periods of no flow when the plant is shutdown. The effluent temperature depends on the time of year and ranges from approximately 25 to 35 degrees Celsius. Two field trips provided temperature readings in the pre-discharge basin of 25 °C in April and 33 °C in July (Evans, unpublished data 1995). There is approximately a 20 degree difference in temperature between the river and effluent at any time of year (Evans, 1996).

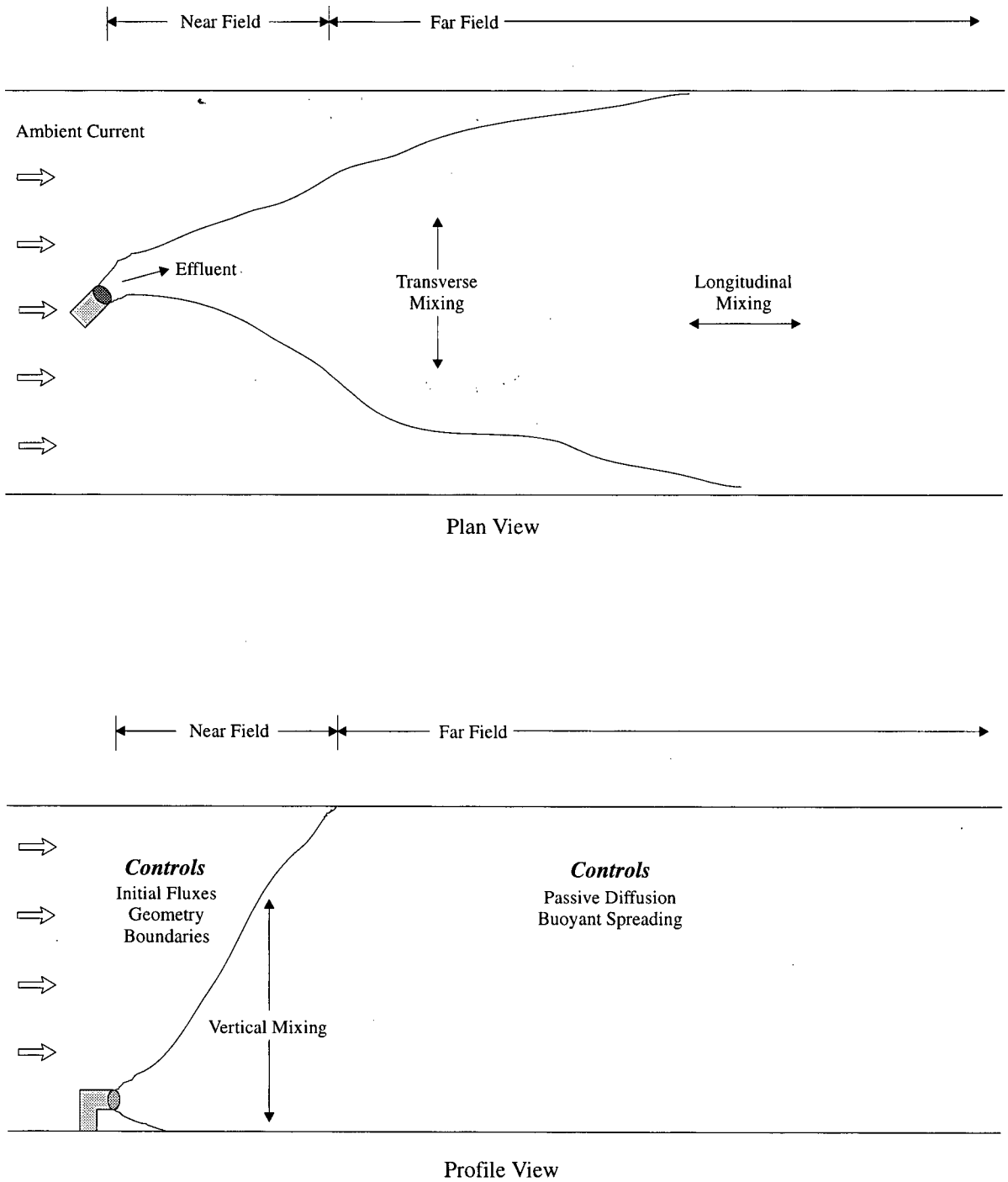

Figure 1. 1: Plan and profile schematics of the near- and far-field mixing zones showing the controlling mixing mechanisms in each zone.

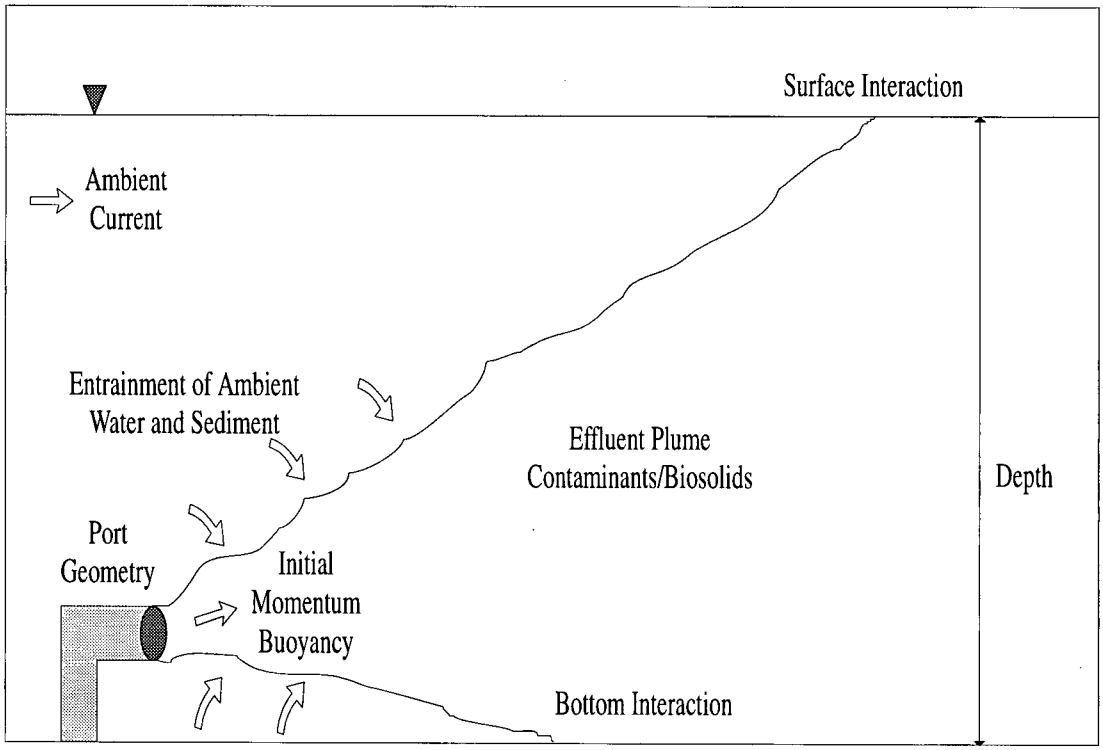

Figure 1. 2: Detailed schematic of the near-field mixing zone describing important parameters and interactions.

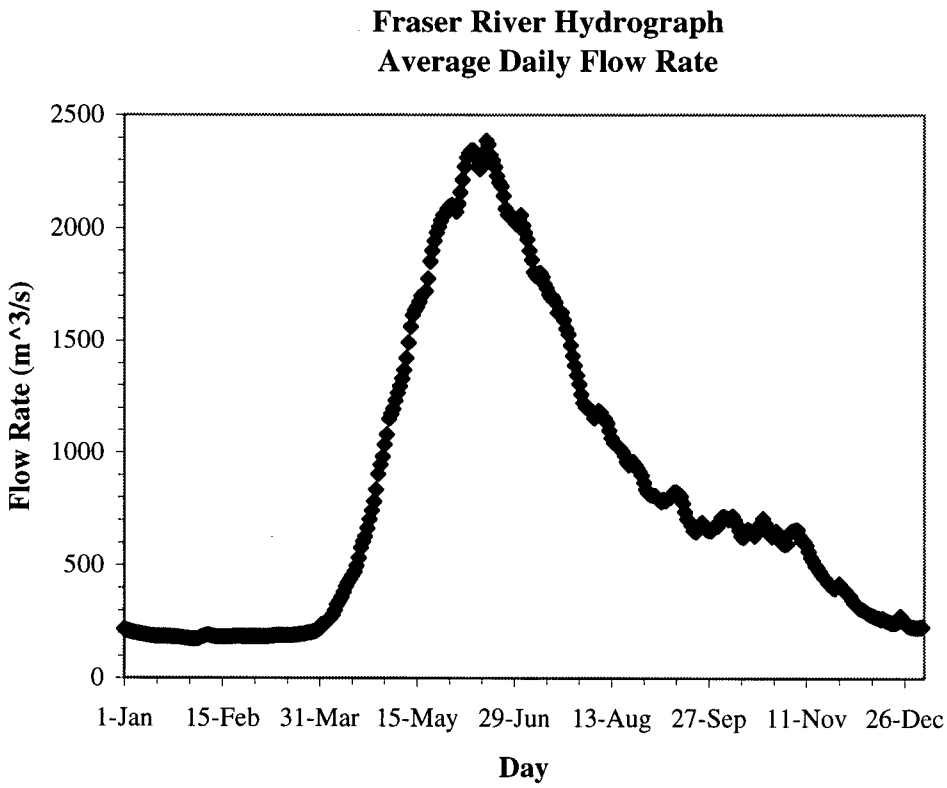

Figure 1. 3: Hydrograph for the Fraser River at the Environment Canada station at Shelly, 20 km upstream of Prince George.

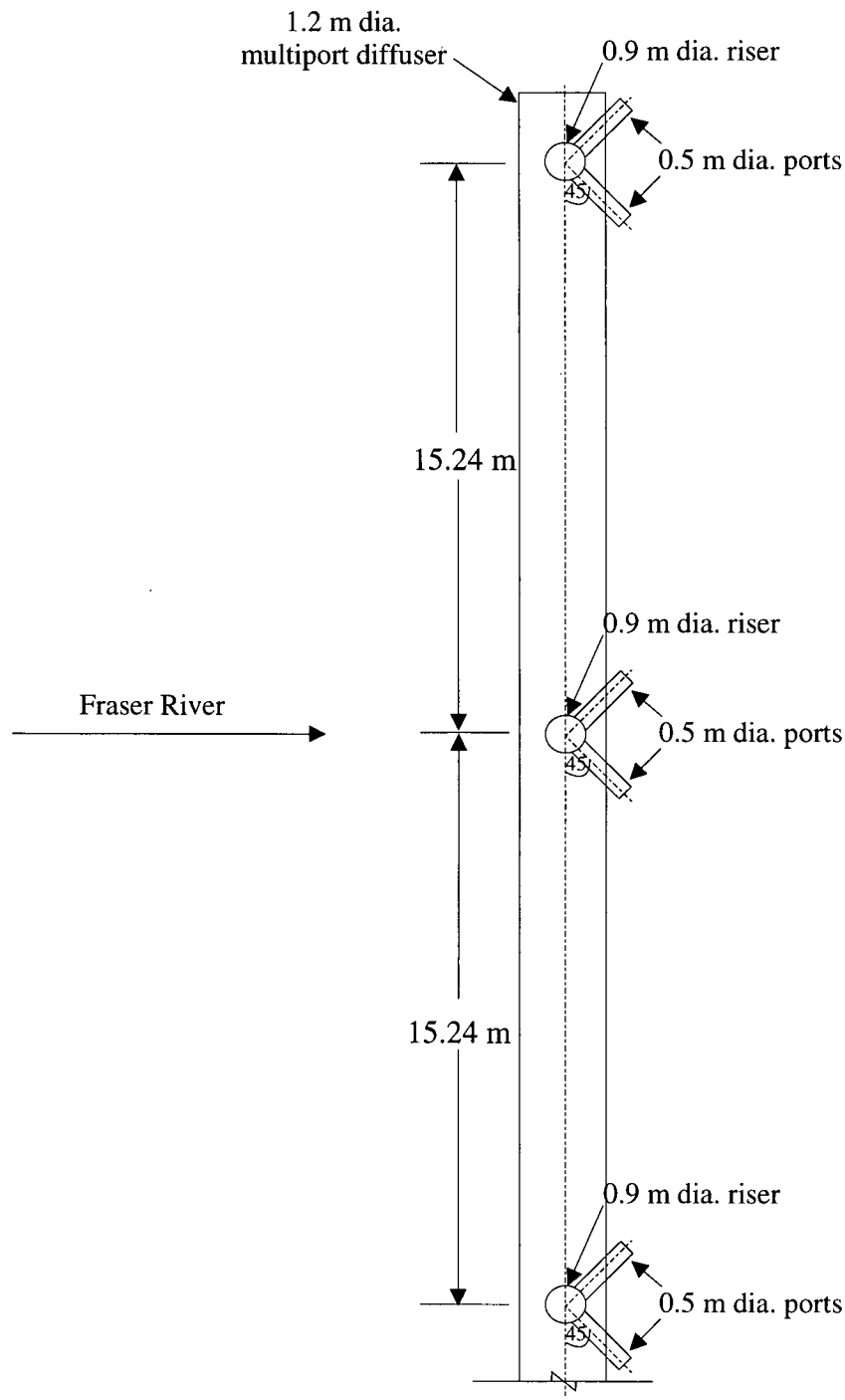

Figure 1. 4: Plan view of the Northwood multiport diffuser structure. Diffuser is oriented perpendicular to the Fraser River and individual ports discharge effluent at 45° to the flow.

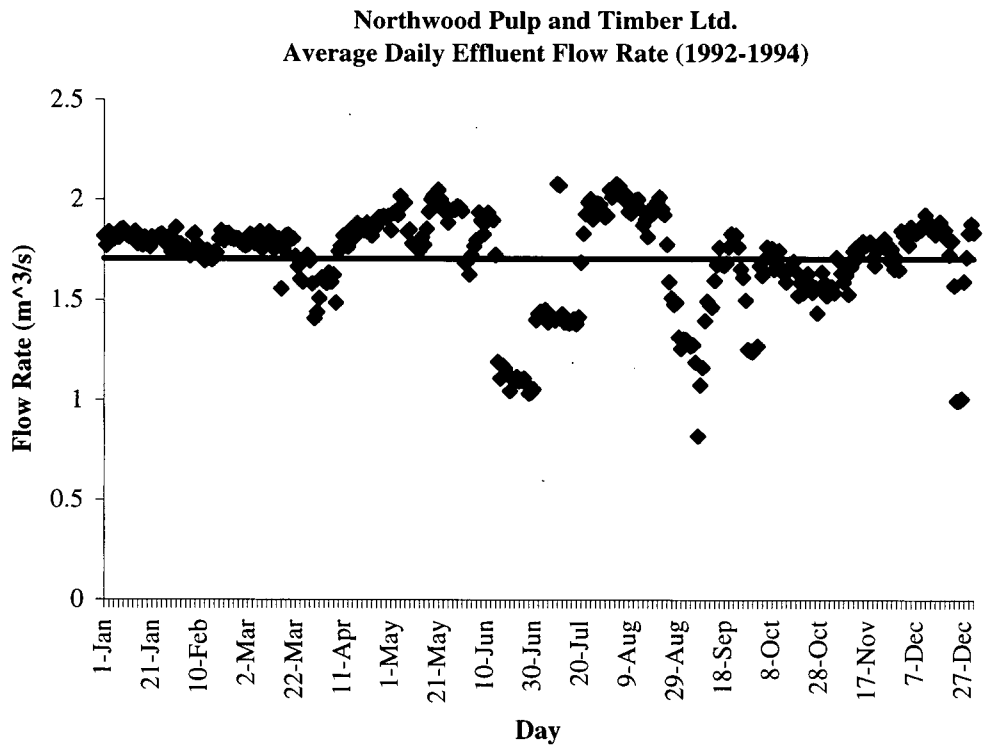

Figure 1. 5: Plot of the average daily effluent flow rate at Northwood for a three year period, data provided by Environment Canada. The solid line is the average monthly effluent flow rate of 1.7 m^3/s.

2.0 LITERATURE REVIEW

Initial dilution of effluent can be effectively accomplished by means of turbulent jets and plumes, since they entrain large amounts of ambient fluid. Turbulent jet behaviour depends on three classes of parameters: jet parameters, environmental parameters and geometrical factors (Fischer *et al.*, 1979). Jet parameters include the initial jet velocity distribution and turbulence level, and the jet mass, momentum and tracer fluxes. Environmental parameters include the ambient conditions of: turbulence levels, currents, and density stratification. Geometrical factors include the jet shape and its orientation plus proximity to boundaries and other adjacent jets. All the above factors will influence the jet behaviour and diluting capability.

This chapter has four sections. The first section describes various basic buoyant jet parameters and concepts. The second section describes length scales which are used to describe flow behaviour. The third section presents relevant previous research and the last section discusses an existing computer mixing zone model.

2.1 Buoyant Jets

A pure jet is a source of momentum only, while a pure plume is a source of buoyancy only. Most discharges have both momentum and buoyancy and are termed buoyant jets. Therefore, a buoyant jet can be considered a source of mass, momentum and buoyancy. The primary variables characterizing a turbulent jet which control dilution are: the mass or volume flux, the momentum flux and the buoyancy flux. The following expressions which describe the jet fluxes were taken from Fischer *et al.* (1979).

The volume flux is

$$\mu = \int_A w dA \tag{2.1}$$

where μ is the specific mass flux or volume flux of the jet, w is the time-averaged jet velocity in the axial direction and A is the cross-sectional area of the jet,

The momentum flux is

$$m = \int_A w^2 dA \tag{2.2}$$

where m is the specific momentum flux.

The buoyancy flux is

$$\beta = \int_A g \frac{\Delta\rho}{\rho} w dA \tag{2.3}$$

where β is the specific buoyancy flux, g is the gravitational constant, ρ is the ambient density and $\Delta\rho$ is the density difference between the jet fluid and the ambient fluid.

For a round jet the initial fluxes of mass, Q, momentum, M, and buoyancy, B, are

$$Q = U_j(\frac{\pi}{4} d^2), \tag{2.4}$$

$$M = U_j Q, \tag{2.5}$$

$$\mathrm{B} = \mathrm{Q}g_o' = \mathrm{Q}(\frac{\Delta\rho}{\rho_a} g), \tag{2.6}$$

where U_j is the absolute jet velocity, d is the port diameter, g_o' is the reduced gravitational constant and $\Delta\rho$ is the density difference and ρ_a is the density of the ambient fluid.

Another governing buoyant jet parameter is the densimetric jet Froude number, which is the ratio of momentum forces to buoyancy forces. The densimetric jet Froude number is defined as

$$Fr = \frac{U_j}{\sqrt{g_o' d}} \tag{2.7}$$

For densimetric jet Froude numbers greater than one, the discharge will initially resemble a jet.

When a buoyant jet is discharged, turbulent entrainment of the surrounding fluid occurs resulting in mixing and dilution of the jet fluid. A shear layer forms between the two fluids of differing densities and velocities. Large billows on the shear layer entrain water into the jet (Fischer, 1979). The shearing flow of the jet breaks down into a turbulent motion as it moves away from the discharge point. As the ambient fluid is entrained into the jet, the internal concentrations are diluted and the jet's width is increased. The term dilution is defined as

$$S = \frac{(C_o - C_b)}{(C - C_b)} \tag{2.8}$$

where C_o is the initial concentration, C_b is the background concentration and C is the concentration at a certain point along the jet.

The flow of a buoyant jet is driven by its excess buoyancy and momentum relative to the ambient fluid into which it is released. The excess buoyancy and momentum will determine the jet's trajectory, velocity, growth and dilution. Usually, the initial jet momentum controls the initial

region of flow behavior, and buoyancy dominates farther away from the source. The combination of initial momentum and buoyancy flux is responsible for turbulent mixing.

2.1.1 Initial Zone of Flow Establishment

Jet behaviour in the near-field has two phases, the Zone of Flow Establishment (ZFE) and the Zone of Established Flow (ZEF). The ZFE is the initial zone where the velocity distribution changes from the port velocity distribution to an axisymmetric jet velocity distribution. After this region, in the ZEF, velocity and concentration values decay from the initial values due to continuous entrainment of ambient fluid. The two regions are shown in Figure 2.1. The time-averaged jet velocity and concentration profiles can be described by a Gaussian distribution in the ZEF (Fischer *et al.*, 1979) as follows:

$$w = w_m \exp[-(\frac{x}{b_w})^2] \tag{2.9}$$

$$C = C_m \exp[-(\frac{x}{b_T})^2] \tag{2.10}$$

where w is the axial velocity, C is the concentration, m refers to the maximum value on the jet axis, x is the transverse distance from the jet axis, b_w and b_T are values of x when w or C reduces to $0.37w_m$ or $0.37C_m$ respectively.

The ZFE is approximately equal to 6 port diameters for a pure axisymmetric jet discharging horizontally. This zone can be as short as 2 to 3 times the port diameter for shallow water conditions (Johnston, 1994) and can also be affected by the densimetric Froude number and the presence of an ambient current (Johnston, 1993). The length of the ZFE decreases with increasing ambient velocity (Chu, 1985). The turbulence intensity on the jet's axis increases in the vicinity of the ZFE zone and then decays with distance from the jet orifice (Fischer *et al.*, 1979).

2.2 Length Scales

Length scales, derived by dimensional analysis, describe the relative importance of discharge fluxes, ambient currents and stratification in controlling behaviour of a buoyant jet (Jirka, 1991). The length scales are calculated from the momentum, buoyancy and volume fluxes of the discharge. The length-scales of importance are as follows, as describe by Jirka (1991).

$$L_Q = \frac{Q_o}{M_o^{1/2}} \tag{2.11}$$

$$L_M = \frac{M_o^{3/4}}{B_o^{1/2}} \tag{2.12}$$

$$L_m = \frac{M_o^{1/2}}{u_a} \tag{2.13}$$

$$L_b = \frac{B_o}{u_a^3} \tag{2.14}$$

where u_a is the mean ambient velocity.

Schematics of the length scales are provided in Figure 2.2 and the following descriptions are from Jirka (1991). L_Q is the discharge or geometric length scale and is a measure of initial jet size and the length of flow establishment in a still ambient environment. For a buoyant jet, L_M is the jet to plume transition length scale and gives a measure of distance over which the transition from jet behaviour to plume behaviour takes place under stagnant uniform ambient conditions. It is a measure of the distance at which the buoyancy becomes more important than the momentum.

In the presence of a cross-flow, L_m, the jet to crossflow length scale, relates the interaction of a momentum-dominated jet with a crossflow. It can be a measure of the distance the jet penetrates

into the ambient environment before the jet is strongly deflected or advected by the cross-flow. Initially the jet momentum controls the jet mixing and trajectory. After the transition, both the jet momentum and ambient current control jet mixing and trajectory. For buoyancy dominated flows, L_b, the plume to crossflow length scale, determines the vertical distance beyond which a plume becomes strongly advected by the cross-flow.

In absence of a crossflow, the jet geometry is important near the source only. For $x << L_Q$, where x is the distance along the jet, the source geometry will have an important effect on the flow behavior. Once $x >> L_Q$, the geometry is unimportant and either the momentum, buoyancy or ambient current will control the flow behaviour. When $x << L_M$, momentum is more important than buoyancy. For $x << L_m$, the jet momentum will dominate and the crossflow will be of secondary importance, while for $x >> L_m$ the ambient current will primarily influence the jet behaviour. The use of length scales to describe important parameters in controlling flow behaviour is summarized in the diagram below.

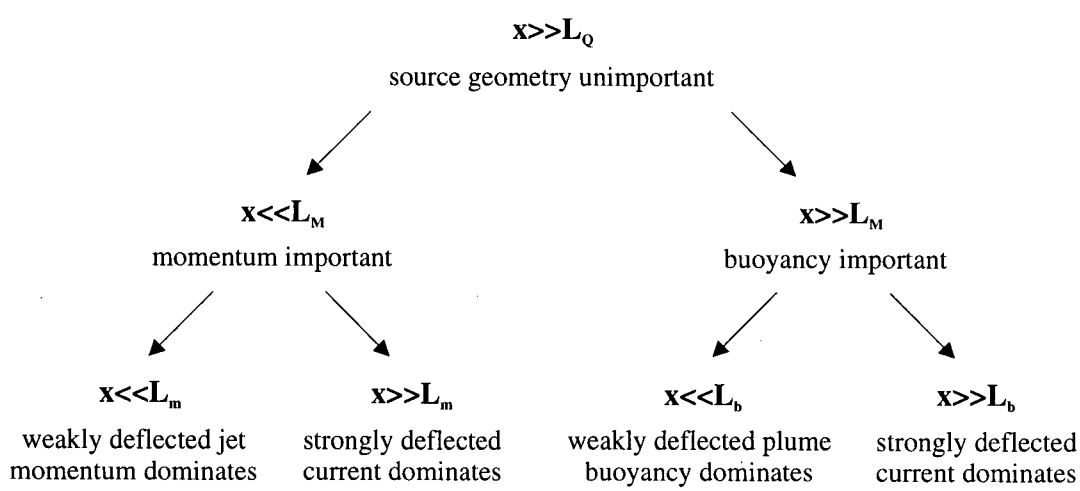

2.3 Previous Experimental Research

Most research on horizontal buoyant jets has been in stagnant ambient environments. Experimental modelling of horizontal buoyant jets in stagnant shallow water has been performed by Sobey (1988) and Johnston (1994). This situation can be adequately modelled by an integral method, in which equations for the conservation of mass and momentum are derived, and dimensional analysis. However, when a jet is impacted by an ambient current or confined by shallowness, the mixing process becomes complicated. Therefore, the integral type of analysis is incapable of predicting the action of an ambient current, the shallow water, re-entrainment of partially diluted fluid, or bottom attachment.

Minimal research has been done in the area of discharging horizontal buoyant jets in shallow water in motion, where shallow water is defined as ambient water depth less than 20 times the port diameter (Lee and Jirka, 1981). Studies by Lee (1987, 1989), Johnston (1993) and Rajaratnam (1995) have examined a buoyant jet entering shallow water in the presence of a crossflow. Shallowness has been shown to restrict dilution and change the cross-sectional shape of the jet (Johnston, 1993). However, the combined effects of (1) boundary interactions, (2) a weak jet discharging into a strong ambient current, and (3) port orientation, relative to the ambient current, on dilution are relatively unknown. Each of these effects will be addressed in turn.

2.3.1 Boundary Interactions

Boundary interactions occur when the jet contacts the upper water surface or the river bottom. The free surface and bed boundaries can both simultaneously impact the dilution of the jet. The interaction with the surface provides a transition between the mixing processes in the near-field and the processes in the far-field. Plume attachment to the bottom is caused by the ambient crossflow or

the entrainment demand of the jet. Bottom attachment is of concern because it can greatly influence the mixing process and have benthic impacts of importance where contaminants are of concern.

Research by Johnston (1994) and Sobey (1988) has shown the tendency of jets to attach to the closest boundary, or the centerline to be attracted towards it, due to the Coanda effect. Coanda attachment is believed to be caused by the pressure difference created by the entrainment of fluid through the surface of the jet closest to the solid boundary, as shown in Figure 2.3 (Wood, 1994). The fluid entrained from below the jet is from a confined area, while the fluid above the jet is from an unconfined area. This results in higher velocities below the jet and thus, lower pressure exists closest to the boundary, a Bernoulli effect, and the buoyant jet moves towards the boundary until clinging takes place. Therefore, the attachment mechanism depends on the pressure distribution on the surface of the jet, which results from the entrainment demand and the increased velocity in the small area below the jet (Wood, 1994).

However, Sobey (1988) showed that the densimetric jet Froude number and initial buoyancy force have minimal affect on jet mixing characteristics compared with the proximity of the free surface and bed boundary. It was shown that closeness to the bottom boundary restricts initial dilution compared with an unconfined environment.

Johnston (1994) studied the influence of the bottom boundary on mixing of a buoyant jet in a shallow, stagnant ambient environment. With higher densimetric jet Froude numbers, there is more of an attraction towards the bed when the closeness to the bed was held constant. When the Froude number is held constant and the bed proximity parameter (Z_o) changed, bed attachment is evident for low values of Z_o. For higher values of Z_o the jet is not affected, and for intermediate values the jet

centerline does not rise or fall. In summary, the distance to the free surface has a minor influence on jet behaviour when compared to bed proximity, and the proximity to the bed has considerable influence of the flow pattern of a buoyant jet.

2.3.2 Ambient Current

A flowing ambient environment complicates the mixing process and the ratio of absolute jet velocity to mean ambient velocity, R, becomes an important mixing parameter. A horizontal buoyant jet in a crossflow has a three-dimensional trajectory which differs from a horizontal jet in a stagnant environment or a vertical jet in a crossflow. The motion in the horizontal plane (x-y) is driven by the jet momentum and ambient current, while the motion in the vertical plane (x-z) is determined primarily by the buoyancy force. Generally, an ambient current will increase dilution because it creates further entrainment of water by forcing ambient fluid through the jet (Tsanis, 1994).

Johnston *et al.* (1993) conducted an experimental study to investigate the mixing processes of a round buoyant jet entering a shallow water in motion. They show that the dilution of a buoyant jet entering shallow moving water is significantly different from one discharging into an unconfined ambient environment. An ambient current increases the dilution and effects the jet's flow structure such that significant differences occur compared to a similar jet in a stagnant fluid.

The cross-sectional shape of a jet changes as it aligns with the current. A jet discharging into a crossflow is asymmetrical about the centerline until it is strongly deflected by the current. Gaskin (1995) investigated entrainment velocities of a buoyant jet in a crossflow and found that as the ambient velocity increased, the entrainment velocities became increasingly asymmetrical. Johnston (1993) found that the current tends to compress the horizontal width of the upstream-side of the jet, while expanding the width of the downstream-side. Furthermore, Johnston (1993) found that as the

current increases, the horizontal penetration of the jet into the ambient water reduces. Ambient currents also affect the path of the jet in the vertical plane and small currents can overcome boundary attachment.

2.3.3 Port Orientation

This section describes the effect of port orientation on dilution relationships derived by previous researchers for a buoyant jet in a crossflow.

Vertical Jets in a Crossflow

Wright (1977) investigated the behaviour of a vertical round buoyant jet in a uniform horizontal crossflow. The primary objective of the research was to predict trajectories of a buoyant jet in a crossflow. The resulting model predicts the vertical rise and dilution of the jet as a function of horizontal position. Four different flow regimes are proposed by Wright which are momentum-dominated near- and far-field (MDNF and MDFF), and buoyancy-dominated near- and far-field (BDNF and BDFF). The near-field is the region where the entrainment process is unaffected by the crossflow.

The regimes depend on the relative importance of the length scales. For example, consider the case $L_M/L_b >> 1$, where the affect of buoyancy is relatively weak compared to the momentum. The higher the ratio, the greater the distance required to generate enough additional momentum due to buoyancy to begin to control the flow behavior. Therefore, the case would be momentum-dominated. The length scale range for each regime is presented in Table 2.1.

Table 2. 1: Description of Flow Behaviour Regime and Length Scale Range

Regime	Length Scale Range	Description
MDNF	$x << L_M$ and $x << L_m$	Strong momentum jet in a weak current
MDFF	$x << L_M$ and $x >> L_m$	Weak momentum jet in a strong current
BDNF	$x >> L_M$ and $z < L_b$	Strong buoyant plume in a weak current
BDFF	$x >> L_M$ and $z > L_b$	Weak buoyant plume in a strong current

For a case involving a weak jet in a strong current, as is the case in the present study, the equations for the momentum-dominated far-field, MDFF, flow regime are relevant. The trajectory and dilution equations are written below and were developed by dimensional analysis, and confirmed by experimental data (Wright, 1977; Fischer, 1979).

$$\frac{z}{L_m} = C_2 (\frac{x}{L_m})^{1/3} \tag{2.15}$$

$$\frac{SQu_a}{M} = C_6 (\frac{z}{L_m})^2 \tag{2.16}$$

where S is the centerline dilution, Q is the jet discharge, M is the initial momentum flux, u_a is the ambient velocity, z is the vertical height and L_m is the jet to crossflow length scale. The coefficients C_2 and C_6 are determined experimentally. The solutions do not consider ambient turbulence and assume self similar concentration profiles and that the crossflow does not affect the dilution equations in the near-field. Wright found that the trajectory coefficients are weakly dependent on the velocity ratio.

Horizontal Jets in a Crossflow

Research on horizontal buoyant jets discharging into a perpendicular ambient current has been examined and compared with vertical jets in a crossflow (Lee and Neville-Jones (1987); Lee (1989); Johnston (1993); Gaskin (1995); Rajaratnam *et al.* (1995)). A horizontal discharge should be

similar to a vertical jet, but the buoyancy of the discharge will affect the initial trajectory and dilution of the jet. A momentum-dominated jet may aligned with the ambient current before significant buoyant rise takes place.

Lee and Neville-Jones (1987) investigated the initial dilution of a horizontal round buoyant jet in a perpendicular crossflow by the interpretation of field and laboratory data. The data correlated well with the power dependence for the vertical jet of Wright's (1977) in the BDNF and BDFF regimes. However, the coefficients were larger than Wright's due to the additional dilution gained with a longer three-dimensional trajectory for a horizontal jet. The research showed that dilution for a horizontal discharge can be 20 to 50 % greater than for a vertical jet for a greater distance along the jet trajectory.

Lee (1989) analyzed Ayoub's (1971) experimental data in which a horizontal momentum-dominated buoyant jet was discharged in a crossflow. The densimetric jet Froude number ranged from 15 to 90 and the velocity ratio ranged from 5 to 20. The power dependence for the trajectory and dilution relationships for the MDFF regime were supported by the data. The trajectory coefficient showed a weak dependence of the velocity ratio.

The results of Johnston (1993) experiments indicated that the dilution data were consistent with the vertical jet of Wright's (1977) and horizontal jet of Lee's (1989) for the momentum dominated regimes. In the experiments performed, the densimetric Froude number varied from 5 to 15 and the velocity ratios from 3 to 20. The dilution data clearly showed the transition between the near- and far-field regimes, with dilution increasing when the jet enters the far-field.

Gaskin (1995) experimentally investigated the behaviour of a single buoyant jet in a stationary and flowing ambient environment. The dilution data corresponded with both the trajectory and dilution equations of Wright (1977), equations 2.15 and 2.16. Gaskin compared her work to research performed by Knudsen (1988) and Wong (1991) and found her dilution to be less for the same distance, approximately half when compared to Wong's data. The explanation for the difference was that Wong's experiments were conducted in an open flume which would result in increased ambient turbulence levels compared with Gaskin's towed port. Gaskin later shows that higher ambient turbulence disrupts the flow structure of the jet and results in increased dilution.

Rajaratnam *et al.* (1995) experimentally studied a horizontal, non-buoyant, turbulent wall jet discharged at right angles to a current. The experiments performed involved a strong jet in a weak current, that is, the jet velocity was greater than the ambient velocity. The experiments showed that the concept of the momentum dominated regime is also applicable to wall jets and the MDFF is more extensive than the MDNF for the range of velocity ratios examined. The data corresponds well with the theory that dilution is proportional to the distance away from source to the 2/3 power and indicates that the constant of proportionality has a dependence on the velocity ratio.

45° Vertical Jet in a Crossflow

Minimal research has focused on jets discharging at a 45° angle to an ambient current, either horizontally or vertically. Chu (1985) investigated oblique vertical jets in a crossflow. For jets with a 45 degree vertical angle, the trajectory and dilution power law (equations 2.15 and 2.16) held constant. The coefficients and rate of entrainment increased for decreasing velocity ratio. The velocity ratios ranged from 2 to 10, with the ambient velocity staying constant at 0.10 m/s. The

entrainment coefficient is dependent upon the velocity ratio and the angle of discharge relative to the current.

Summary

The momentum dominated far-field regime equations 2.15 and 2.16 can be transformed into one equation by substituting the trajectory equation into the dilution equation for z/L_m.

$$\frac{SQu_a}{M} = C_6 C_2^{\,2} \left(\frac{x}{L_m}\right)^{2/3} \tag{2.17}$$

Substituting in for Q and M and assigning the variable α equal to $C_6 C_2^{\,2}$, equation 2.17 becomes

$$\frac{S}{R} = \alpha \left(\frac{x}{L_m}\right)^{2/3} \tag{2.18}$$

where S is the minimum dilution, R is the velocity ratio, x is the distance downstream and α is an experimental coefficient.

Previous research involving the momentum dominated far-field regime is summarized for the various coefficients in Table 2.2. The power dependence in equations 2.15 and 2.16 for vertical jets hold true for horizontal jets, but the dilution coefficient are generally higher. Also, in the experiments where the jet is stationary instead of towed, the coefficients tend to be higher, possibly due to elevated ambient turbulence levels. In summary, dilution is proportional to the downstream distance to the 2/3 power law for a momentum-dominated jet in a perpendicular crossflow.

Table 2. 2: Summary of the Dilution Coefficient α from Previous Research

Researcher	Jet Type	C_2	C_6	$\alpha = C_2C_6^2$	Range of R
Wright (1977)	V	1.6-2.1	0.14	0.36 - 0.62	
Chu (1985)	45° V	$1.8\cos^{1/3}\theta$	$0.2\cos^{1/3}\theta$	0.52	R = 2-10
Lee (1989)	H	1.69-1.91	0.32	0.91 -1.17	R = 5-20
Knudsen (1988)	H	1.6	0.41	1.05	
Wong (1991)	H	1.4	0.56	1.1	
Gaskin (1995)	H	1.3	0.29	0.49	R = 1

Research has not been performed on horizontal buoyant jet discharging at angles other than perpendicular or parallel to an ambient current. Also, there are limited studies involving low velocity ratios or when the ambient velocity is stronger than the jet velocity. The experiments performed in the present study investigate whether the dilution relationship applies to a buoyant jet in a strong ambient current, with a horizontal port orientation of 45 degrees and close proximity to the bottom boundary. In previous research, the dependence of the velocity ratio on the experimental coefficient has not been considered in detail. This study will attempt to quantified the relationship between the velocity ratio and dilution for a weak jet in a strong ambient current.

2.4 Modelling of Near-field Mixing

There are generally two types of mathematical models to predict dilution of a jet: integral and length scale models (Tsanis, 1994). Integral models can be further divided into Eulerian and Lagrangian. Eulerian models determine dilution by calculating the amount of entrained mass using a set of ordinary differential equations, which describe the rate of change of various parameters with respect to the jet's centerline. Lagrangian models follow the plume element throughout its trajectory with respect to time. Changes in plume properties are determined in adjacent elements at each time increment.

Length scale models are derived through dimensional analysis. They describe the relative importance of discharge, momentum flux, buoyancy flux, ambient crossflow and density stratification in controlling flow behaviour (Jirka and Doneker, 1991). Cornell Mixing Zone Expert Systems, CORMIX, is a length scale based model. It uses a hydrodynamic-flow-classification scheme based on length scales to determine the near-field behaviour of the discharge configuration. CORMIX has three submodels, CORMIX 1, 2 and 3. CORMIX 1 is used for submerged single-port discharges, CORMIX 2 for submerged multiport diffusers and CORMIX 3 for surface discharges. Detailed information on CORMIX can be found in the paper by Jirka and Doneker (1991).

2.4.1 Introduction to CORMIX 1

Based on inputs of geometry and dynamic characteristics of the submerged single-port discharge and ambient environment, CORMIX 1 classifies the discharge configuration into one of 35 generic flow classes. The classification is based on criterion involving dimensionless length-scale variables and empirical coefficients. The length scales previously defined in Section 2.2 are calculated from the momentum, buoyancy and volume flux of the discharge.

There are four major flow behaviour categories within CORMIX 1. Discharges into stratified ambient environments are designated as S class flows. V, vertical, and H, horizontal, class flows are buoyant jets in an uniform ambient environment. Negatively buoyant discharges are defined as NV and NH class flows in an uniform ambient environment. Lastly, A class flow behaviour is for bottom attached flows. A flow chart for V and H class flows is provided in Figure 2.4 and flow charts for other classifications are found in Jirka and Doneker (1991).

Bottom attached flows are divided into two different classes, wake attachment and Coanda attachment. Wake attachment is caused by the presence of the discharge outfall structure

interrupting the ambient velocity field and producing a region of recirculation. If the effluent intrudes far enough away from the boundary, wake attachment will not occur. The criterion for wake attachment to occur is:

$$(L_m + h_o) \leq L_Q \tag{2.19}$$

and

$$(L_b + h_o) \leq L_Q \tag{2.20}$$

An additional criterion to determine if the plume remains attached to the bottom or lifts off is based on the plume's buoyancy is:

$$\frac{L_b^2}{L_Q L_m} > S_R(\frac{f}{8})^2 \tag{2.21}$$

where S_R is the recirculation factor and f is the ambient flow Darcy-Weisbach friction factor.

Coanda attachment depends on the vertical angle of discharge and initial jet width. The criterion for attachment is:

$$\tan\theta_o < (0.2 - h_o / L) \tag{2.22}$$

where L is equal to L_M for weak crossflows and L_m for strong crossflows, and θ_o is the vertical angle of the jet.

There are two tiers to the CORMIX 1 computer model. The first tier consists of data input by the user, parameter and length scale calculations and then flow classification. The second tier performs detailed calculations of plume trajectory, position, width and dilution using a control volume concept.

Version 3.1 of CORMIX has a post-processing option which allows a jet integral model called CORJET to be run after CORMIX has been run for a specific case. CORJET solves a three dimensional round jet integral equation for a single submerged buoyant jet which will predict near-field dilution only. CORJET can be used after CORMIX 1 has predicted stable, non-attached flows. The module assumes a infinite receiving water body without any boundary effects. The theory behind CORJET is based on Jirka and Fong (1981).

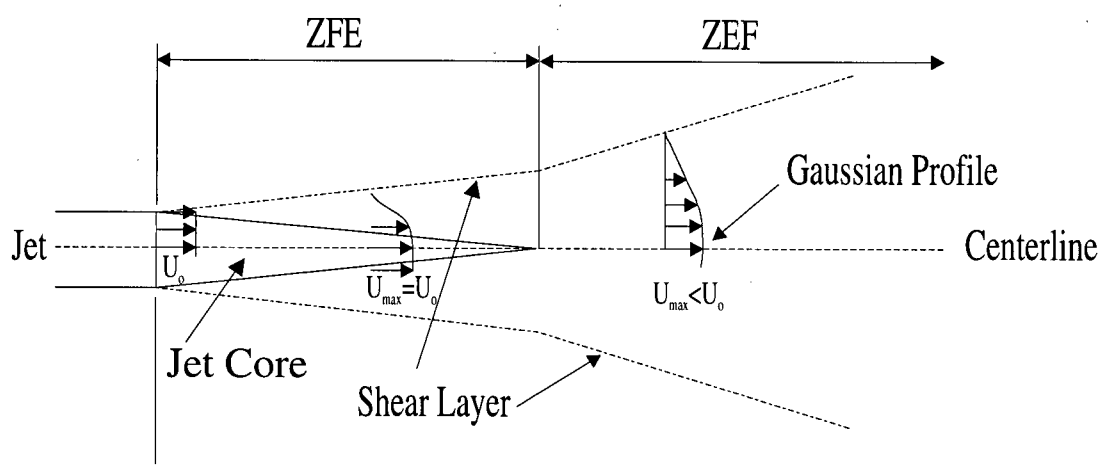

Figure 2. 1: The initial jet discharge zone encompasses the zone of flow establishment, ZFE, and the zone of established flow, ZEF.

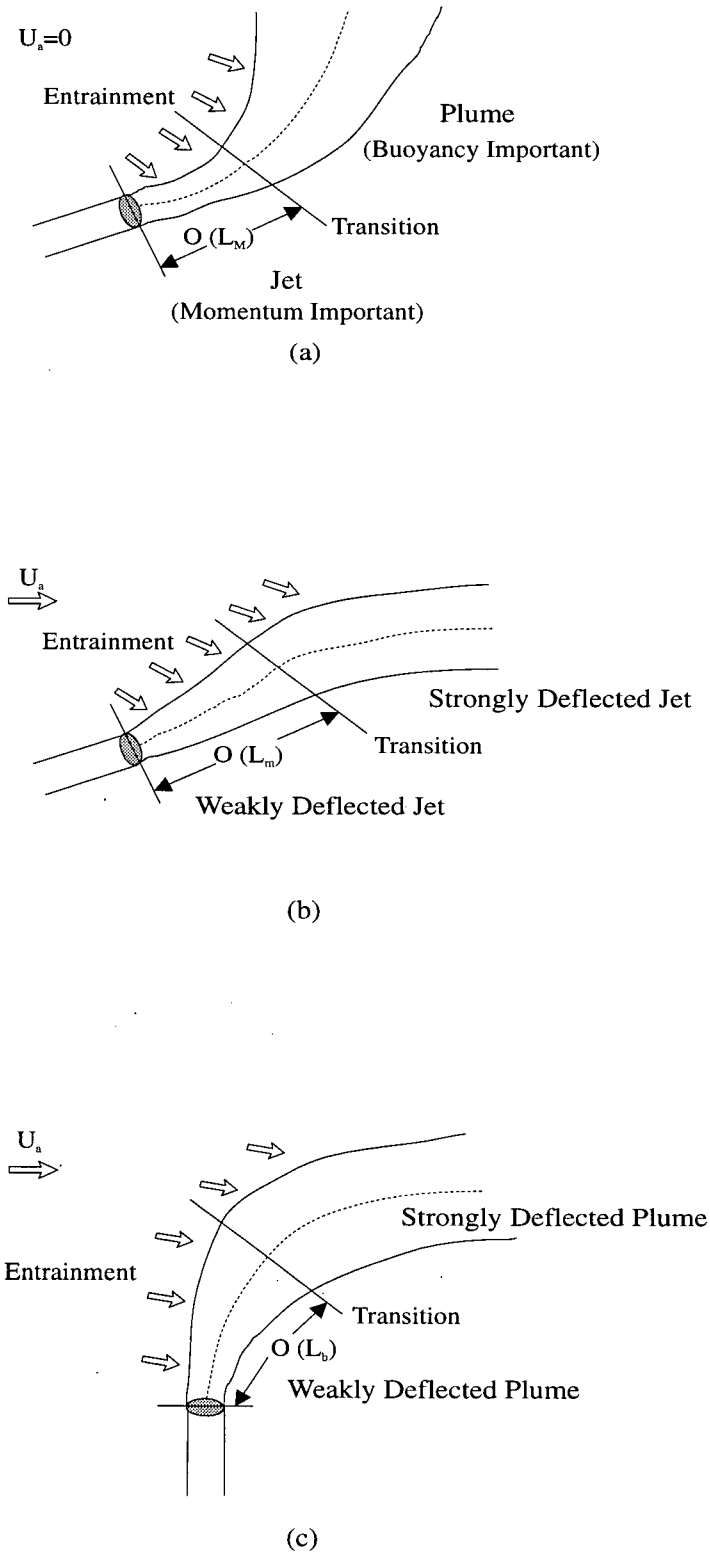

Figure 2. 2: Length scale schematics: (a) jet to plume length scale, (b) jet to crossflow length scale, (c) plume to crossflow length scale.

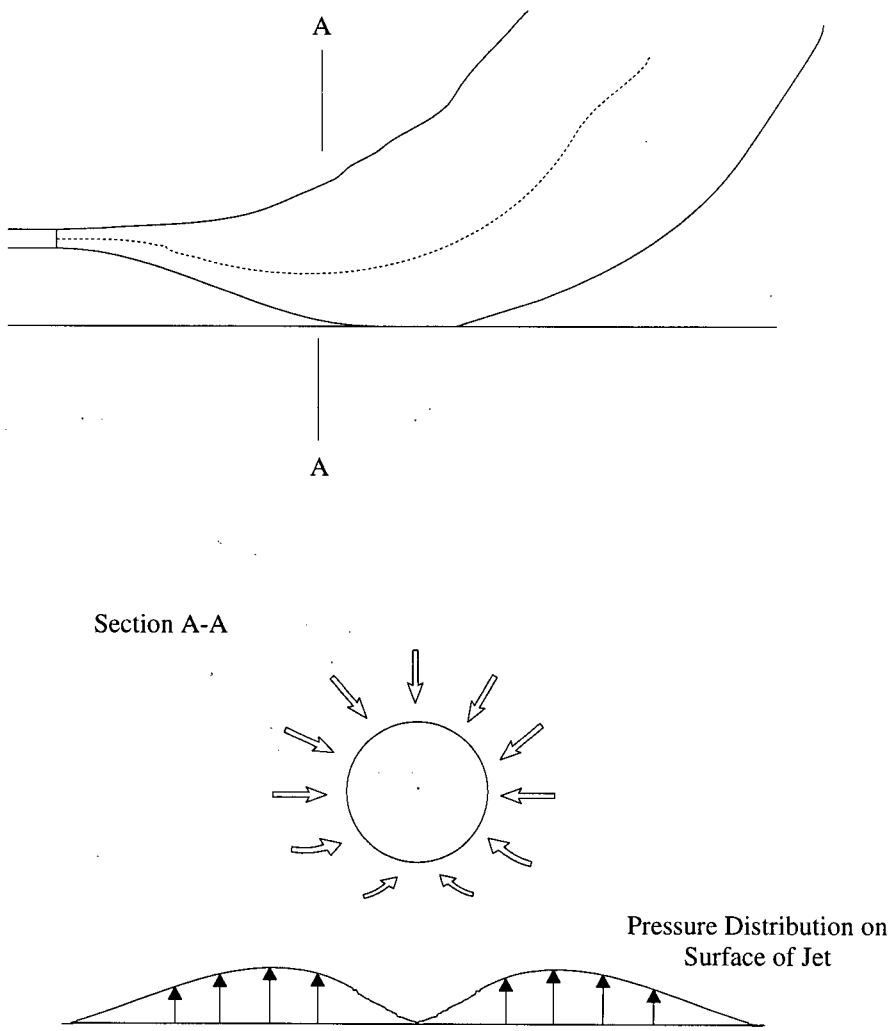

Figure 2. 3: Coanda attachment is caused by the pressure distribution and entrainment demand of the jet (Wood, 1994). Higher velocities exist below the jet and the lower pressure by Bernoulli's' effects cause the jet's centerline to move towards the boundary.

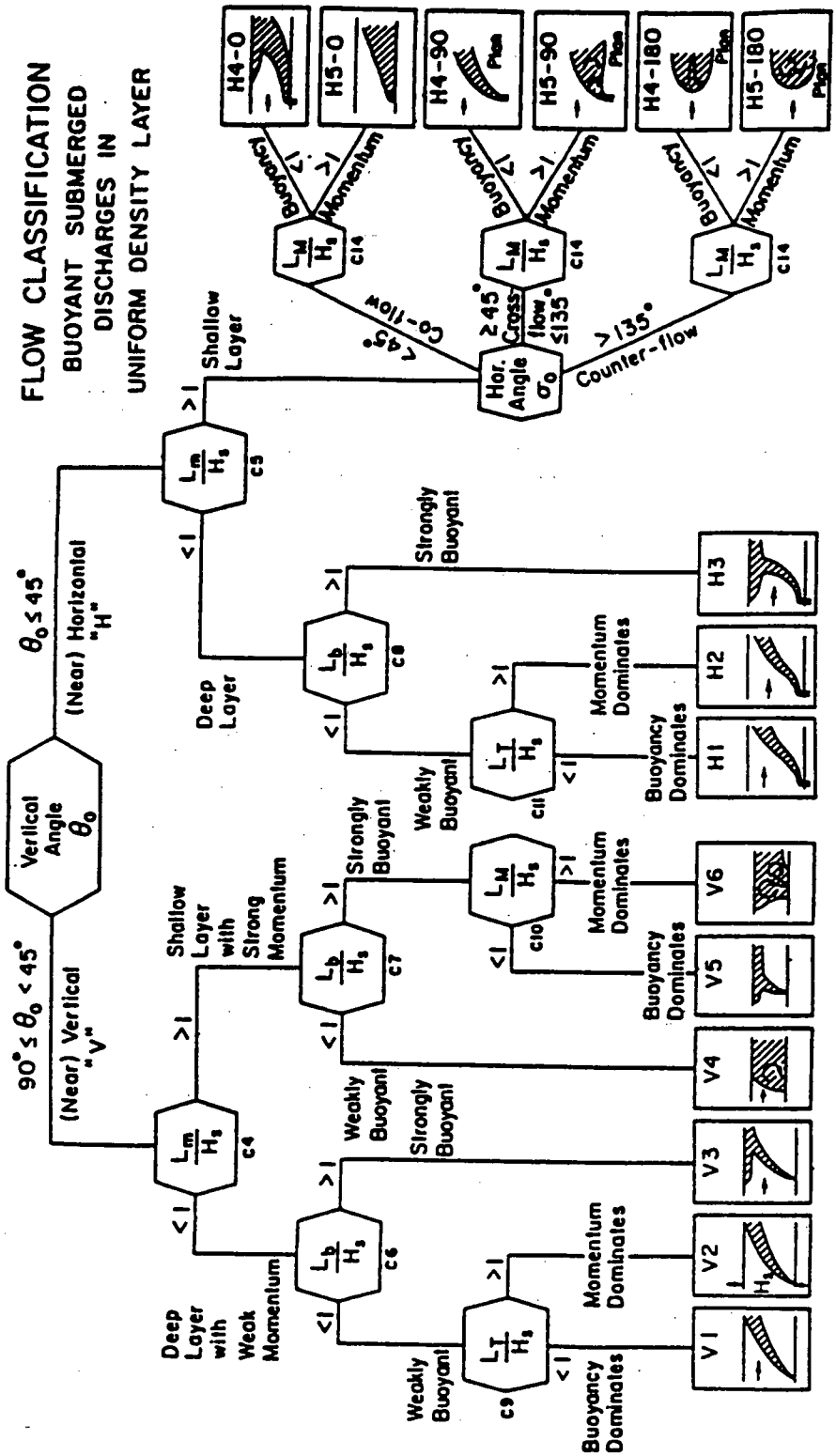

Figure 2. 4: Flow classification chart for CORMIX 1 mixing model (Jirka and Doneker, 1991). Chart is for horizontal or vertical discharges in an uniform density ambient environment.

3.0 LABORATORY EXPERIMENTS

The ports on the Northwood multiport diffuser can be treated as single, horizontal, positively buoyant turbulent jets discharging into a moving ambient environment, prior to the merging of individual jets. Laboratory experiments modelling a single Northwood port have been performed to investigate the affects of a high ambient current, shallow water depth and port orientation, as well as changes in ambient and discharge parameters on dilution and other jet parameters.

The range of densimetric jet Froude number, Fr, and the ratio of absolute jet velocity to mean ambient velocity, R, were preserved in the laboratory experiments. These were the two modelling parameters that varied between the laboratory experiments. By varying these parameters, a range of possible conditions were modelled to simulate seasonal changes in velocity and temperature at Northwood and in the Fraser River. Froude numbers would be higher in the winter than summer, since colder temperature in the river would increase the ambient water density. Velocity ratios are highest in the winter when the flow in the river is low, and lowest in the spring when the flow is high.

Approximate velocity ratios based on monthly flow records from Northwood and the Fraser River are provided in Table 3.1. The flow records for Northwood were provided by Environment Canada. The ambient velocity in the Fraser River, U_a, is calculated based on the assumption of a rectangular channel and the flow rates at the Shelly station. The jet velocity, U_j, is calculated assuming equal flow through the six ports of the Northwood diffuser. Field data for temperature are presented in Table 3.2 (Evans, unpublished data, 1995) to show variations in parameters for different seasons.

Table 3. 1: Monthly Values of R Based on the Northwood Port Velocity, U_j and Fraser River Velocity, U_a

	Fraser River			Northwood		
	Q	Average Depth	Ua	Q	Uj	R
Month	(m^3/s)	(m)	(m/s)	(m^3/s)	(m/s)	(Uj/Ua)
January	190	1	0.6	1.8	1.5	2.4
February	183	1	0.6	1.8	1.5	2.5
March	197	1	0.7	1.7	1.5	2.2
April	607	1.8	1.1	1.8	1.5	1.3
May	1743	3.4	1.7	1.9	1.6	0.9
June	2200	3.9	1.9	1.4	1.2	0.6
July	1571	3.2	1.6	1.6	1.4	0.8
August	984	2.4	1.4	1.9	1.6	1.2
September	725	2	1.2	1.5	1.2	1.0
October	653	1.9	1.1	1.6	1.4	1.2
November	457	1.5	1.0	1.7	1.4	1.4
December	254	1.1	0.8	1.7	1.5	1.9

Notes:

1) Flow rate, Q, data is from Environment Canada station at Shelly (see Figure 1.3).

2) U_a is calculated assuming the river is represented by a rectangular channel with an average width of 300m in the vicinity of the diffuser. Depth is calculated by Manning's formula.

3) U_j is calculated by dividing the flow rate by the number and area of ports, where the port diameter is 0.5m.

4) These values were used to calculate a general range of velocity ratios only.

Table 3. 2: Seasonal Changes in Parameters at Northwood Based on Field Data and Environment Canada Data

Season	Ua	Uj	Ta*	Tj*	R	Fr
Winter	0.7	1.5			2.2	
Spring	1.1	1.5	4	25	1.4	12.5
Peak	1.9	1.2			0.6	
Summer	1.6	1.4	13	33	0.9	9.2
Fall	1.1	1.4			1.2	

* From field measurements - April 16&17, July 25-August 4, 1995 (Evans, per.comm.).

3.1 Experimental Design

The range of the velocity ratios and Froude numbers were based on average conditions at Northwood and in the Fraser River. The port velocities for the experiments ranged from 0.32 to 0.46 m/s and the ambient velocities from 0.31 to 0.47 m/s, providing a range of velocity ratios from 0.8 to 2.4. The Froude numbers varied from 8 to 15. Details of the experimental parameters are provided in Table 3.3. For each experiment, the experimental parameters given are the temperature of the effluent and ambient, T_j and T_a, the ambient velocity, U_a and the jet discharge, Q_j. The calculated values in the table are the reduced gravity, g_o', jet velocity, U_j, velocity ratio, R, and Froude number, Fr. A generalized schematic of the experimental parameters is shown in Figure 3.1.

Table 3. 3: Details for Each Experiment

Exp #	Tj Celsius	Ta Celsius	go' (m/s^2)	Ua (m/s)	Qj (lpm)	Uj (m/s)	R Uj/Ua	Fr Uj/(go'd)^.5
1	46.0	12.0	0.095	0.33	4.2	0.40	**1.20**	**10.5**
2	46.4	13.9	0.094	0.38	4.9	0.46	**1.22**	**12.3**
3	45.2	12.9	0.091	0.38	4.0	0.38	**0.99**	**10.2**
4	47.9	17.0	0.096	0.44	4.6	0.43	**0.99**	**11.4**
5	48.6	15.2	0.102	0.31	3.4	0.32	**1.03**	**8.2**
6	48.2	15.2	0.100	0.38	3.4	0.32	**0.84**	**8.3**
7	43.1	10.9	0.085	0.47	4.4	0.42	**0.88**	**11.6**
8	42.8	8.9	0.085	0.45	3.8	0.36	**0.80**	**10.0**
9	41.5	9.4	0.080	0.21	4.5	0.42	**2.02**	**12.3**
10	42.4	12.8	0.080	0.25	5.5	0.52	**2.08**	**15.0**
11	41.7	13.9	0.076	0.27	4.2	0.40	**1.47**	**11.7**
12	42.9	9.7	0.085	0.16	4.1	0.39	**2.42**	**10.8**

Notes:

1) Diameter of port is equal to 1.5 cm for all experiments.
2) Water depth for all experiments is approximately equal to 9 cm.
3) Distance of port above flume bottom is 1.75 cm.
4) Jet Reynolds numbers ranged from approximately 8400 to 12000.
5) Flume Reynolds numbers ranged from approximately 14000 to 37000.
6) Percentage of error in velocity measurements is approximately ± 5%.
7) Error in temperature measurements is approximately ± 1 degree Celsius.

The diameter of the model port is 1.5 cm and hence, the length scale ratio is

$$d_r = \frac{d_p}{d_m} = \frac{0.5}{0.015} = 33\,1/3$$

This means that the laboratory lengths are 33 and a third times smaller than at Northwood. The port size and length scale were constrained by the flume width. Both the jet and flume Reynolds number are in the turbulent range, greater than 4000. The depth of the water in the flume was approximately 9 cm corresponding to a three meter water depth in the river. The port center is 1.75 cm from the flume bottom and was scaled using the length scale and original drawings of the diffuser design in 1960, provided by Northwood. The actual port height may be lower or higher depending on the season and over time erosion and deposition of sediment may occur around the diffuser.

3.2 Physical Set-up

The experiments were performed in a recirculating laboratory flume in the hydraulics lab of the Civil Engineering Department at UBC. The flume was of width 0.5 m, height 1.0 m and length 15 m. A PVC port was placed in the center of the flume, approximately 3 m away from the flume inlet, at an angle of 45 degrees to the flow oriented to the left in the downstream direction (Figure 3.2).

The buoyancy flux was created by discharging hot water from a constant-head tank above the flume, through the port into the cooler moving flume water. The jet velocity was controlled by a valve at the bottom of the tank and set by a rotameter below the port outlet. A line of T-type thermocouples were used to measure the temperature across the flume at different depths and locations down the flume. The flume water temperature was approximately 30 degrees warmer than the discharge for all experiments.

The line of thermocouples were moved vertically by a transversing mechanism that accurately measured the vertical distance from the flume bottom. A thermocouple measured changes in voltage. A data acquisition system collected the voltage readings which were converted to a temperature-time series using linear calibration curves (Appendix A). The curves were developed by submerging the thermocouples in a water bath of known temperature and recording the voltage. The user interface of the computer program shows continuous temperature readings for the individual thermocouples, while the acquired data is stored as a temperature-time series.

3.3 Experimental Procedure

Once the temperature of the ambient and discharge were initially read with the thermocouples, the absolute jet velocity was used to set the desired Froude number for the experiment. From the jet velocity and a desired velocity ratio, the ambient velocity was determined and set using an Ott Mechanical Current Meter. The line of thermocouples was positioned at the first transect and data was recorded at 5 Hz. The length of data record was set at 1024 points in order for the time-averaged temperature values to be relevant. The recording frequency was limited by the data acquisition and computer set-up.

Once measurements at all the desired vertical positions were taken, the traversing mechanism was moved to the next downstream location. The thermocouples were spaced at 1 cm apart across (y-direction) the flume starting at 14 cm from the left flume wall. The vertical (z-direction) spacing was 1 cm after the 0.5 and 1.0 cm measurements from the bottom boundary. The number of vertical measurement locations varied with each experiment and distance downstream. The downstream (x-direction) stations were generally at 2, 3, 4, 6, 8, 10, 15 cm from the port outlet. This enabled a three dimensional temperature grid to be produced.

3.4 Ambient Characterization

It is important to know the height of the bottom boundary layer to see whether the port centerline is discharging into the boundary layer. Using the Sontek 3-D acoustic doppler velocimeter (ADV), measurements of three typical mean velocities in the flume were taken at the port location. The results have been plotted in Figure 3.3, as measurement height over total water depth (Z/D) versus time-averaged velocity over the mean velocity. The mean velocity and shear stress of each experiment were determined by a least-squares method of regression of the log-velocity law. Due to the limitations of the ADV, it was impossible to record measurements above Z/D around 0.25. Thus, the full extent of the boundary layer could not be measured. However, it can be seen that the port centerline is within the boundary layer at approximately U/U_a of 95 %.

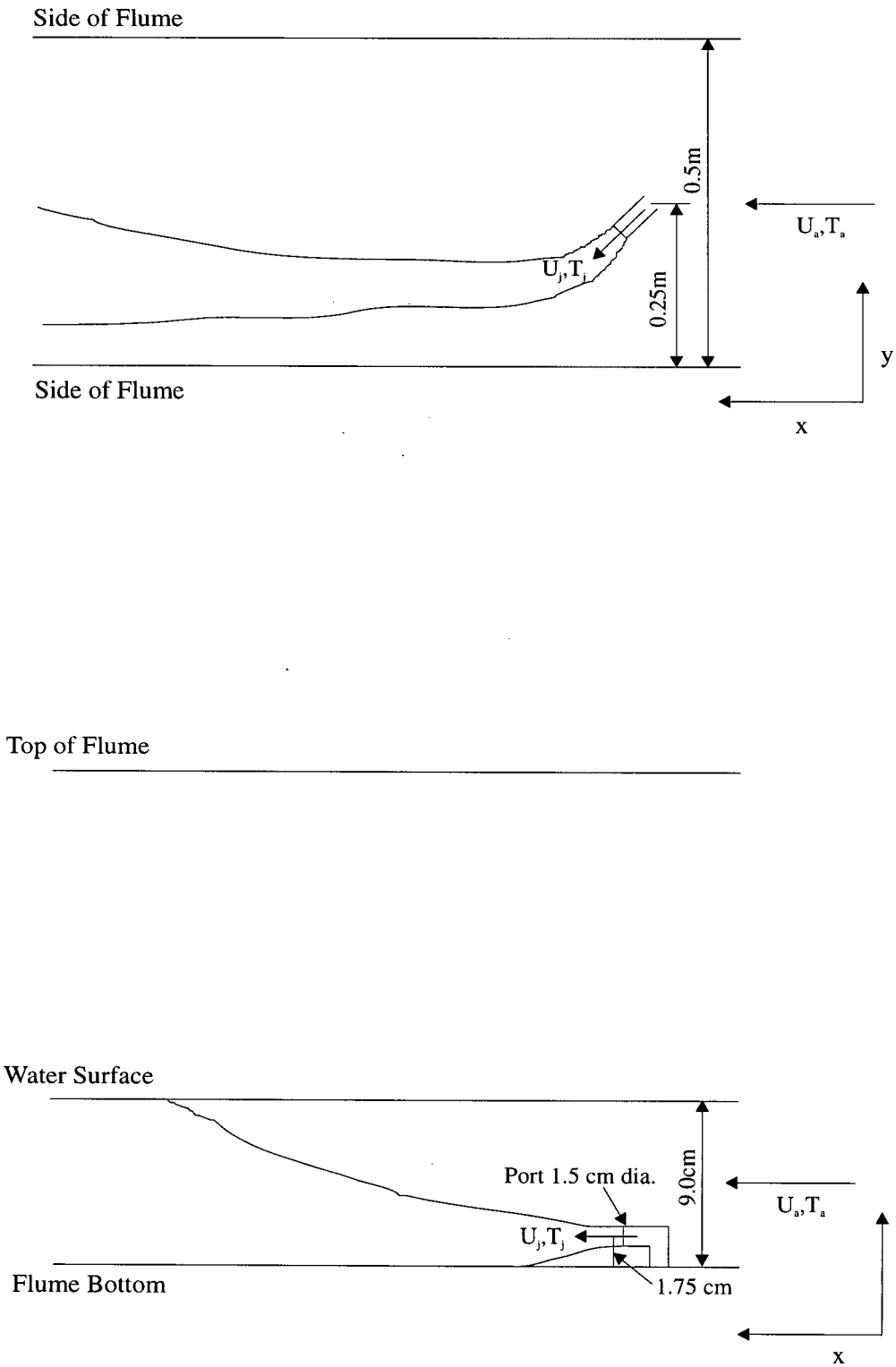

Figure 3. 1: Plan and profile schematics of the general experimental set-up describing the important parameters and dimensions.

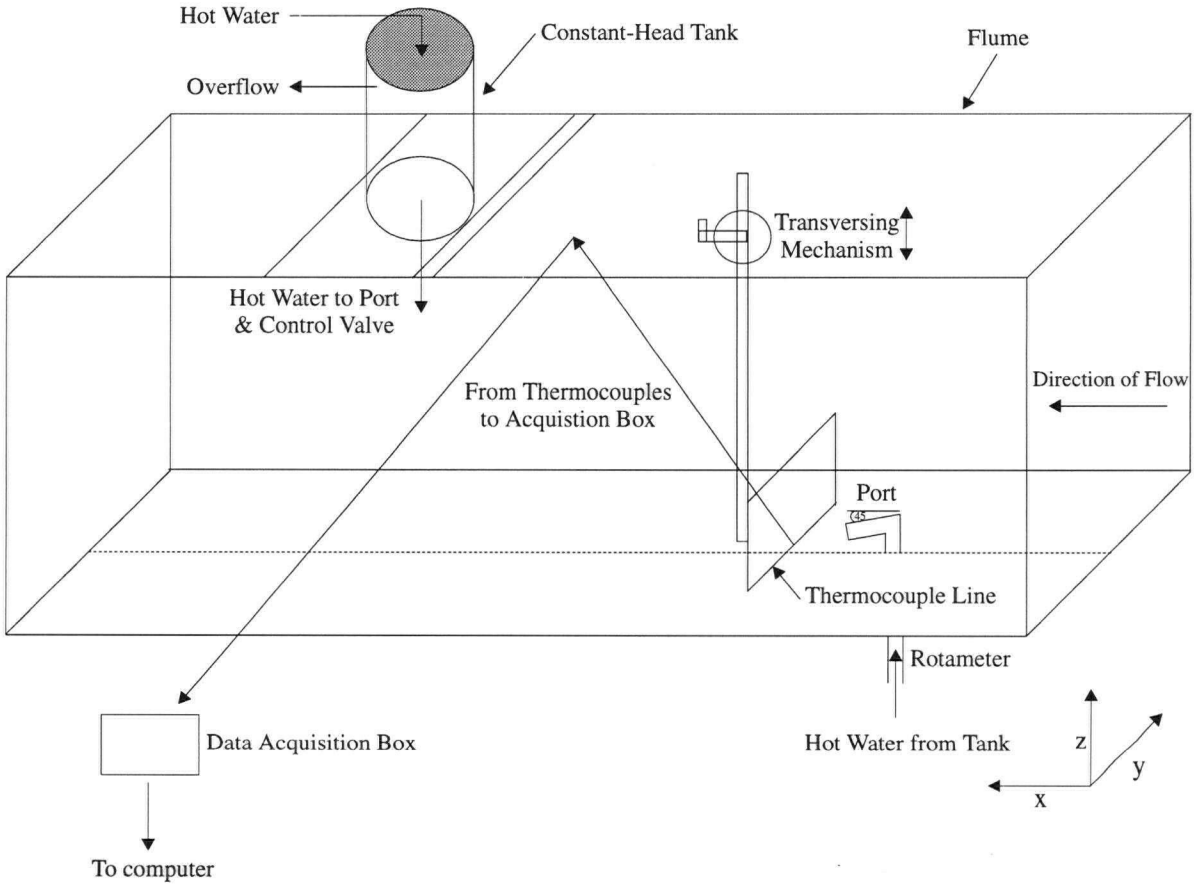

(a)

(b)

Figure 3. 2: Details of the experimental configuration (a) Schematic (b) Photograph

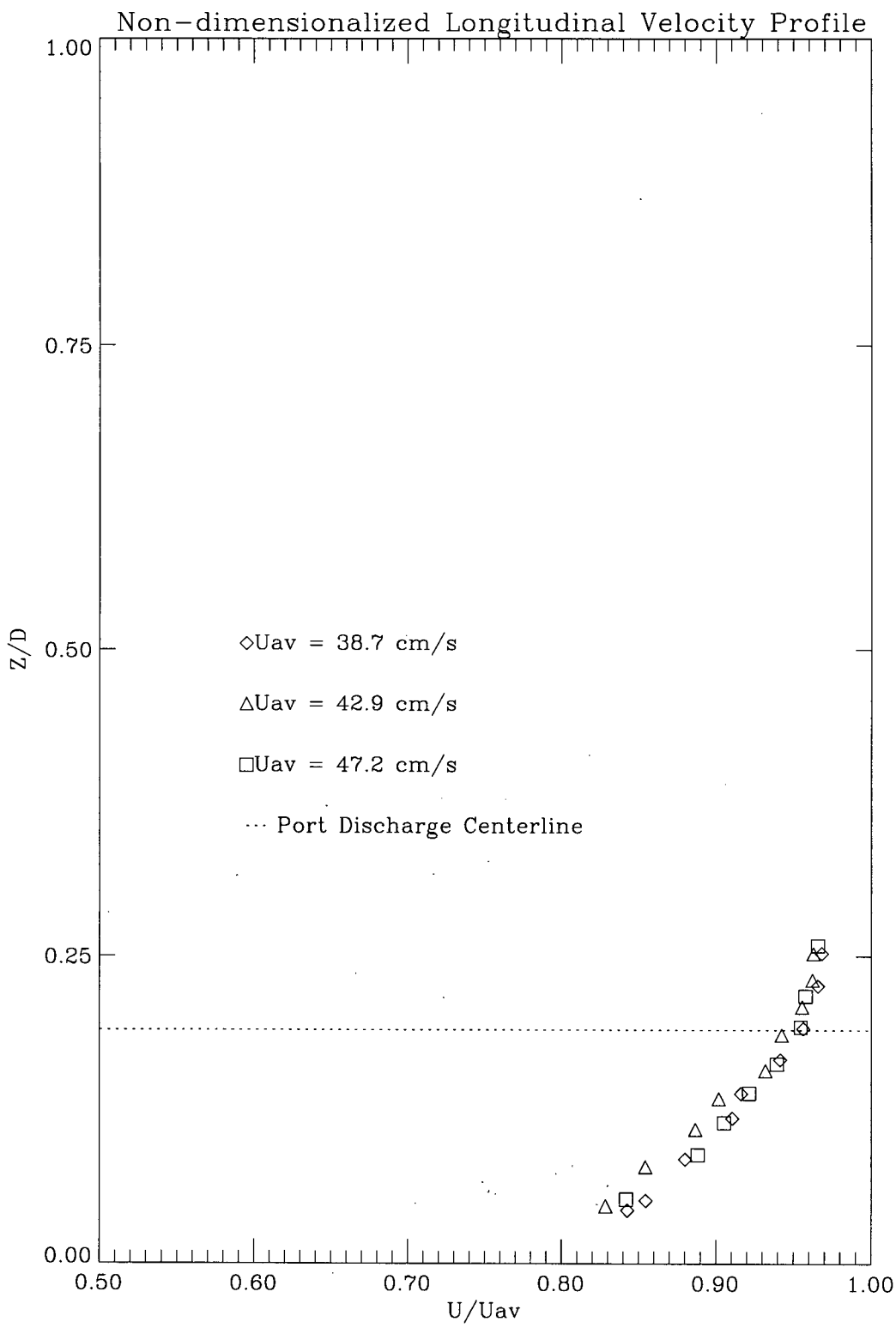

Figure 3. 3: Ambient velocity characterization of the laboratory flume to show port is discharging into the top of boundary layer.

4.0 RESULTS, ANALYSIS AND DISCUSSION OF DATA

The temperature data obtained from the experiments were used to calculate dilution, estimate jet trajectory and turbulence intensity as a function of downstream distance. Experiments 1 to 8 (see Table 3.3) can be considered to model a weak jet in a strong current, since the component of the jet velocity in the direction of the ambient current is less than the ambient velocity, $U_j\cos\theta < U_a$, where θ is the angle of discharge relative to the current. The component velocity of the jet for experiments 9 to 12 is greater than the ambient velocity. The initial mixing entrainment mechanisms are impacted by whether the jet component velocity is less or greater than the ambient velocity. If the jet velocity is less than the ambient velocity, the jet will be advected by the current, whereas if the jet velocity is greater, the jet will be dragged until the velocities are equal.

The length scales L_Q, L_M, L_m and L_b have been calculated and summarized in Table 4.1 for all experiments. Since $L_M >> L_b$, the flow behaviour of the jet for all experiments should be initially momentum dominated. Since the last data set is collected at x = 15 cm which is on order of L_M, there should be no buoyancy effects on dilution in the vicinity of the port. Between 10 to 15 cm, buoyancy will start to become more important than momentum. For most experiments the range of x is greater than L_m and therefore, the discharge should resemble a strongly deflected jet with the flow behaviour controlled by the ambient current. The length scale values indicate that the majority of the dilution data should fall within the momentum dominated far-field, MDFF, flow regime.

Table 4. 1: Length Scales for Experiments 1 to 12

Exp #	Lm (cm)	LM (cm)	x/LM (range)
1	1.6	14.8	0.14 - 0.68
2	1.6	17.3	0.12 - 0.58
3	1.3	14.4	0.14 - 1.04
4	1.3	16.1	0.12 - 0.93
5	1.4	11.6	0.17 - 1.30
6	1.1	11.7	0.17 - 1.28
7	1.2	16.5	0.12 - 0.91
8	1.1	14.2	0.14 - 1.06
9	2.7	17.4	0.12 - 0.86
10	2.8	21.2	0.09 - 0.71
11	2.0	16.6	0.12 - 0.90
12	3.2	15.3	0.13 - 0.98

Notes:

1) Length scale L_Q is equal to 1.3 cm for all experiments.
2) Length scale L_b is very small and ranges from approximately 0.006 to 0.14 cm.

4.1 Dilution

A minimum and mean dilution were calculated from the recorded temperature data using the following equations.

$$S_{min} = \frac{T_j - T_a}{T_{max} - T_a} = \frac{\Delta T_o}{\Delta T_{max}} \tag{4.1}$$

$$S_{mean} = \frac{T_j - T_a}{T_{avg} - T_a} = \frac{\Delta T_o}{\Delta T_{avg}} \tag{4.2}$$

where T_j is the hot water temperature, T_a is the flume water temperature, T_{max} is the maximum time-averaged temperature at that x location and T_{avg} is the calculated average temperature across the jet. To calculate T_{max}, the data is time-averaged for each thermocouple at each z location and stored in a two-dimensional array in the yz plane. The maximum value is then determined which is

representative of the jet centerline temperature. This gives an approximate minimum dilution at a certain x location. The average temperature of the jet was calculated by defining the jet edge to be 1% of the maximum excess temperature (T_{max} - T_a) at that x location. Therefore, an average temperature is calculated by summing the temperature excess recorded by an individual thermocouple multiplied by the area that the thermocouple represents and then dividing by the total average area, as follows:

$$T_{avg} = \frac{\sum \Delta T_i A_i}{A_T} \tag{4.3}$$

where ΔT_i is the time-averaged temperature difference for a thermocouple at the center of the cell, A_i is the area of the cell and A_T is the total area of the jet.

4.1.1 Dilution for Varying Froude Number and Velocity Ratio

As shown by the calculated length scales, buoyancy should have minimal effect on dilution. This is supported by comparing dilution as a function of downstream distance for experiments with different Froude numbers, but similar velocity ratio, as shown in Figure 4.1a. The two sets of lines are for minimum and mean dilution calculations and the different symbols are for the different experiments. For the range of Froude numbers examined in the study (Fr = 8 to 15), there is little affect on dilution. The slight variations in mean dilution are probably because the velocity ratios are not exactly the same. No trend can be seen in the plot, thus implying the momentum forces are more important than the buoyancy forces.

Dilution as a function of downstream distance for varying velocity ratio but similar Froude number is shown in Figure 4.1b. As expected, dilution increases with decreasing velocity ratio. The minimum dilution does not start to vary between experiments until x > 6cm. The trend in initial

dilution, concerning changes in velocity ratio or ambient current, is better shown by the mean dilution data. Generally, dilution should be greater for increasing ambient velocity, decreasing jet velocity and decreasing velocity ratio. The experimental data indicates that for the range of conditions examined, the velocity ratio has a greater influence on dilution than the Froude number.

4.1.2 Non-Dimensional Dilution

A plot of minimum dilution against *x* non-dimensionalized by L_m is provided in Figure 4.2a for the upper and lower limits of the velocity ratio examined, R = 2.4 and R = 0.8. The data points for the two experiments when $x < L_m$ and $x > L_M$ deviate from the 2/3 slope of the MDFF regime (solid and dashed line on plot). For example, experiment #12's value of L_m is approximately 3.2 cm and therefore, the data from *x* stations less than 3.2 should not fall on the line, which are the first two points (x = 2cm and x = 3cm). The last point (x = 15 cm) for experiment #8 is greater than L_M and also does not fall on the line. Therefore, the area of interest on the graph for all experiments is between values of x/L_m of 1 and 10.

Minimum dilution versus x/L_m for all experiments is shown in Figure 4.2b. Since the Froude number is unimportant, experiments with approximately the same velocity ratio can be grouped together. The 2/3 slope fits the data well within the length scale limits for the MDFF regime, that is $x > L_m$ and $x < L_M$. The plot also shows the dependence of the velocity ratio on dilution and on the coefficient α in the dilution relationship for the momentum dominated far-field regime,

$$\frac{S}{R} = \alpha\left(\frac{x}{L_m}\right)^{2/3} \tag{4.4}$$

The coefficient α was calculated using the method of least squares regression for each experiment (Table 4.2) assuming a slope of 2/3. Only the data points that are within the length scale limits for the MDFF were used to calculate the coefficient (see x range column of Table 4.2). The coefficient is higher compared to previous research and varies with the velocity ratio, increasing with decreasing R values.

Table 4. 2: Values of Coefficient α for Experiments 1 to 12

Exp #	α	x range	R	Fr	Ua	Re(a)
1	1.04	3 - 10	1.20	10.5	0.33	24484
2	1.03	3 - 10	1.22	12.3	0.38	29677
3	1.16	2 - 10	0.99	10.2	0.38	28241
4	1.14	2- 15	0.99	11.4	0.44	37138
5	1.13	2 - 10	1.03	8.2	0.31	24746
6	1.28	2 - 10	0.84	8.3	0.38	30602
7	1.26	2 - 15	0.88	11.6	0.47	35318
8	1.29	2 - 10	0.80	10.0	0.45	35526
9	0.9	3 - 15	2.02	12.3	0.21	17625
10	0.91	3 - 15	2.08	15.0	0.25	18580
11	0.96	3 - 15	1.47	11.7	0.27	20289
12	0.77	4 - 10	2.42	10.8	0.16	13838

A plot of α against velocity ratio is shown in Figure 4.3. The best fit line for the variation in the coefficient α with velocity ratio is

$$\alpha = 1.16R^{-0.41} \tag{4.5}$$

Combining equations 4.4 and 4.5, the dilution relationship becomes

$$S = 1.16R^{0.59}\left(\frac{x}{L_m}\right)^{2/3} \tag{4.6}$$

There may be many reason for the variation in α with R and from previous research. When R is decreasing, the ambient velocity and Reynolds number are increasing which will change the jet trajectory and produce higher levels of ambient turbulence. The jet trajectory aligns with the current direction more quickly with increasing ambient velocity. Gaskin (1995) also showed that higher ambient velocities increase the level of ambient turbulence and hence, increase dilution. The values of ambient Reynolds number, ambient velocity and jet Froude number in Table 4.2 have been plotted against R (Figure 4.4) to see if any trend emerges with respect to these parameters on the coefficient. The coefficient α is provided for each point. No trend is visible in the data for why α varies exponentially with R.

The port diameter, proximity to the bed and angle of discharge are other factors which could have an effect on the coefficient and thus, the difference from previous research. The coefficient may have some dependence on the angle of discharge because the 45 degree angle of discharge produces initial momentum in both the x and y direction, whereas for a 90 degree discharge the initial momentum is in the y direction only. Overall, the minimum dilution data supports the relationship for the MDFF, that is, the dilution is proportional to the downstream distance to the 2/3 power. The mean dilution data shows a similar trend as minimum dilution where the coefficient α increases with decreasing velocity ratio.

4.1.3 Comparison with CORMIX 1 Output

The computer mixing model CORMIX has been run for each of the experiments to determine its usefulness in predicting near-field dilution. For all 12 experiments, the flow class is determined to be H2 which is defined as horizontal, weakly-buoyant, momentum-dominated jet behaviour. Additionally, experiments 3 to 7 are A1 class flows and experiment 8 was A2 class flow behaviour indicating bottom attachment with and without lift-off, respectively. The type of attachment

predicted by CORMIX is wake attachment, not Coanda attachment. Since attachment to the bottom boundary is predicted, the recirculation module is applied to calculate dilution.

The experiment data for minimum dilution and equation 4.4 are compared to dilution predicted by CORMIX in Figure 4.5 and Figure 4.6. When the velocity ratio is greater than one, CORMIX predicts no bottom attachment, experiments 1, 2 and 9 through 12 (Figure 4.4). CORMIX 1 underestimates the minimum dilution, but as the velocity ratio becomes greater or the ambient velocity less, the difference between predicted and observed reduces. CORMIX 1 may not be able to account for the increase in turbulence with increasing ambient velocity and thus, would be unable to predict reasonable dilution when turbulence induced by a strong ambient current is a controlling mixing mechanism.

For experiments where recirculation is predicted, which are experiments 3 through 8 when the velocity ratio is less than one, CORMIX 1 overestimates the initial dilution as seen in Figure 4.5. CORMIX 1 does predict higher dilution for decreasing velocity ratios, as the experimental data shows.

Also, CORMIX 1 does not correspond to experimental data on trajectory and width calculation in the initial dilution region. Comparison with experimental data reinforces the idea that CORMIX 1 is not suitable for precise near-field modelling of initial dilution when conditions of shallow water due to closeness of boundaries and strong ambient velocities exist. However, general trends correspond to experimental data and attachment predictions correspond to what was visually seen during the experiments.

4.2 Temperature Contour Plots

Contour plots of time-averaged temperature excess, that is the temperature above the ambient temperature, have been developed in the vertical (yz) plane at different downstream locations. A typical contour plot series (experiment #7) for experiments 1 through 8 is provided in Figure 4.7. Each window is a further downstream (x) location. These plots show the loss of temperature with distance as the jet entrains ambient water leading to dilution. The first vertical measurement is taken 0.5 cm from the flume bottom and it can be assumed that the jet is contacting the bottom. This has an implication with respect to the Fraser River and Northwood since this is an interaction between pulp mill effluent and deposited sediments. There is the possibility of entrainment of bottom sediments into the jet which will transport them further downstream.

The contour plots show the jet's progression from the source. The jet expands horizontally and vertically with each frame, and slowly moves upwards due to the buoyancy. The plume center is skewed due to the effects of boundary closeness, the initial angle of discharge and the ambient current. The upstream-side (left) of the jet is less dilute than the downstream-side (right), resulting in closer contours on the left-side of the plots. The current and angle of discharge causes a non-symmetrical contraction and expansion of the jet. The cross-sectional shape changes as the jet aligns with the current. The current leads to a faster growth rate on one-side of the jet than the other.

To compare the affect of a strong ambient current, Figure 4.8 shows a series of contour plots for a case where the ambient current is weak (experiment #9). In Figure 4.7, the ambient current is 0.47 m/s and in Figure 4.8 the ambient current is 0.21. The jet velocity and the Froude number are approximately the same for both experiments. The jet is larger in both the horizontal and vertical

directions for experiment 9, indicating that the higher current restricts plume growth. Both contour series tend to show the jet being of an elliptical shape, probably due to the closeness of the boundaries limiting the entrainment on the top and bottom.

4.3 Jet Centerline Trajectory

The jet trajectory is highly three dimensional and is controlled by momentum in the y and x direction and by buoyancy in the z direction. The jet has an initial 45 degree horizontal trajectory and in absence of a current would continue on this path. In the presence of a strong ambient current, the jet is quickly advected in the direction of flow. The centerline values are calculated from a weighted average of the time-averaged temperature data, using the expressions.

$$Y_{cl} = \frac{\Sigma(y\Delta T)}{\Sigma\Delta T} \tag{4.7}$$

$$Z_{cl} = \frac{\Sigma(z\Delta T)}{\Sigma\Delta T} \tag{4.8}$$

where y and z are the position of the thermocouple in the transverse and vertical directions respectively and ΔT is the corresponding temperature difference. The values are depth and width averaged.

The calculated horizontal jet trajectory for experiments 1 through 8 is shown in Figure 4.9. The port origin is at 22 cm from the flume wall at x equal to 0 cm. The plot shows that the jet penetrates farther into the ambient water with higher velocity ratios. The higher the ambient current the quicker the jet becomes advected and becomes parallel to the ambient flow. As the current

increases, the horizontal penetration of the jet into the ambient water reduces, but at the same time the higher the Froude number the farther the jet penetrates due to the its greater initial momentum. The jet aligns with the current before it significantly begins to rise due to buoyancy, indicating a momentum-dominated flow.

The current strongly affects the path of the jet in the vertical plane (Figure 4.10). The port origin in the vertical, at x = 0, is 1.75 cm from the bottom. The first recorded x location is 2 cm from the port. The vertical centerline is initially attracted towards the bottom boundary, but as the outlet structure loses its control, or at the end of the ZFE, the centerline begins to rise due to the positive buoyant nature. The initial dip in the centerline trajectory may be representative of Coanda attachment, which occurs with high Fr numbers and close proximity to the bed. The jet will attach to the bottom when initial momentum is controlling and then lift-off, as the buoyancy influence takes over control. The strong current restricts the rise of the jet in the vertical plane as seen by the two different plots. For the experiments where the ambient current is smaller, the length of centerline attraction towards the flume bottom is shortened and the trajectories rise towards the surface more quickly, so that vertical mixing is faster.

4.4 Concentration Profiles

Depth averaged concentration profiles in the horizontal plane, where concentration is the inverse of the dilution, have been plotted in Figure 4.11. The two plots are for different experiments with the same jet velocity but differing ambient velocities. The different symbols are for different downstream locations. For both plots, the peak C/C_o value decreases with distance and the curves are slightly skewed towards the current side of the jet. Therefore, the concentration profile has a slightly non-Gaussian profile in the initial dilution zone due to the discharge angle and ambient

current. Furthermore, a smaller ambient current leads to an increase in the horizontal width of the jet.

Vertical concentration profiles have been developed, see Figure 4.12. These profiles represent the maximum concentration measured at a certain x location. Comparing the plots, there is a greater attachment to the bottom boundary with the higher ambient current, as seen in Figure 4.12a. This is of importance in relation to the Fraser River because of the impact to benthic community and a possibility of turbulent entrainment of bottom sediment into the plume. In Figure 4.12b, the vertical profiles are more representative of a Gaussian shape and have greater vertical jet widths. This indicates that a jet in a weak current is faster to vertically mix than a weak jet in a strong current.

4.5 Temperature-Time Series

The data records are stored as a temperature-time series. Maximum turbulence intensity calculated from the temperature-time series data has been plotted against downstream distance in Figure 4.13. Turbulence intensity is the standard deviation of the temperature fluctuations and is non-dimensionalized by the maximum average temperature at the same location. Turbulence intensity when calculated from velocity data initially increases to a maximum value, on order of 0.1 for x/L_Q equal to 10, and then decays as the jet enters the ZEF (Fischer *et al.*, 1979). Most experiments show an slight initial rise and decay of turbulence intensity. The maximum turbulence intensity values are on order of 0.1.

Since mixing is dominated by the turbulence produced by the interaction between the jet and crossflow, an increase in turbulence should cause an increase in dilution. Turbulence intensity is of interest in relation to this study because higher intensities would cause more collisions between

sediment and biosolids, resulting in the greater possibility of flocculation (Evans, 1996). In general, turbulence intensities are slightly higher for stronger ambient currents as seen in the two different plots in Figure 4.13. This would suggest that when the flow rate is high in the spring, there would be a greater chance of flocculation occurring than at other times of the year. This is also the time when the river transports most of the sediment load.

Turbulence intensity profiles have been produced in the horizontal plane by depth averaging the values for thermocouples within the jet. A typical series for experiments 1 to 8 is provided in Figure 4.14 (experiment 3). The width of the turbulent zone is increasing with distance downstream, as well as the peak values decreasing as expected by theory. The profiles are slightly skewed. The peak in the plots corresponds to where the current impacts the jet, indicating an area of greater temperature fluctuation. Gaskin (1995) also showed this trend.

For experiments 9 to 12, a typical series has been plotted in Figure 4.15 (experiment 12). The experiments 3 and 12 have the same jet velocity. When the current is smaller, there tends to be two peaks on either side of the jet, the higher peak on the left-side of the jet where the current first impacts the jet. Also, there is a greater width of turbulence with decreasing ambient velocity. Turbulence intensity calculated from a temperature-time series is reasonable since the outline of the jet is present and values are similar to intensity calculated from a velocity-time series.

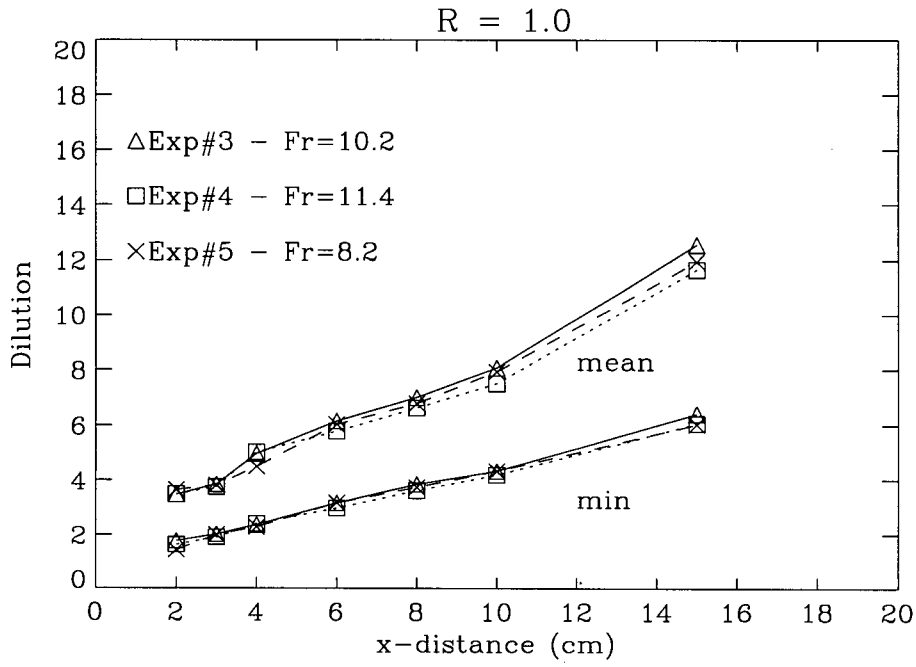

(a)

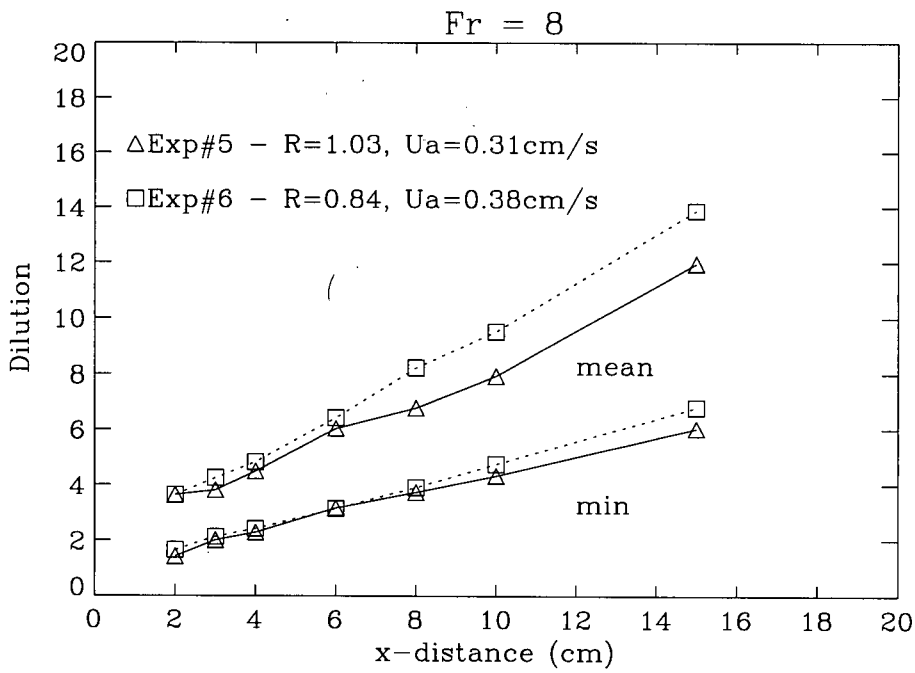

(b)

Figure 4. 1: Dilution with downstream distance (a) for varying Froude number but similar velocity ratio (R=1) and (b) for varying velocity ratio but similar Froude number (Fr=8). The Froude number has minimal influence on the initial dilution, since jet flow behaviour is moment-dominated. Minimum dilution increases with decreasing velocity ratio as expected.

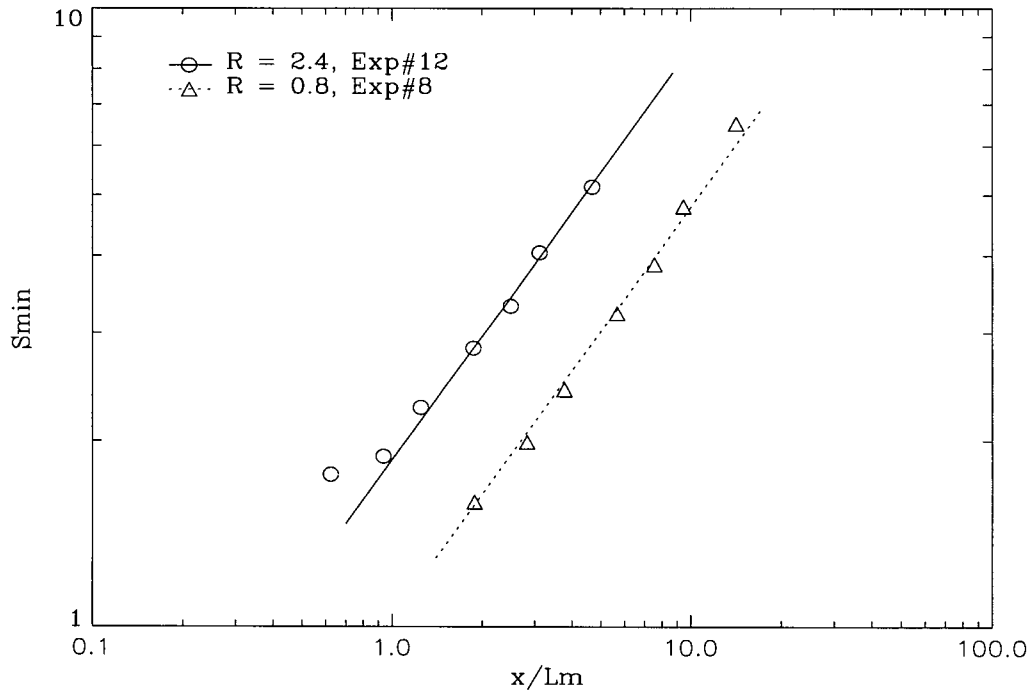

(a)

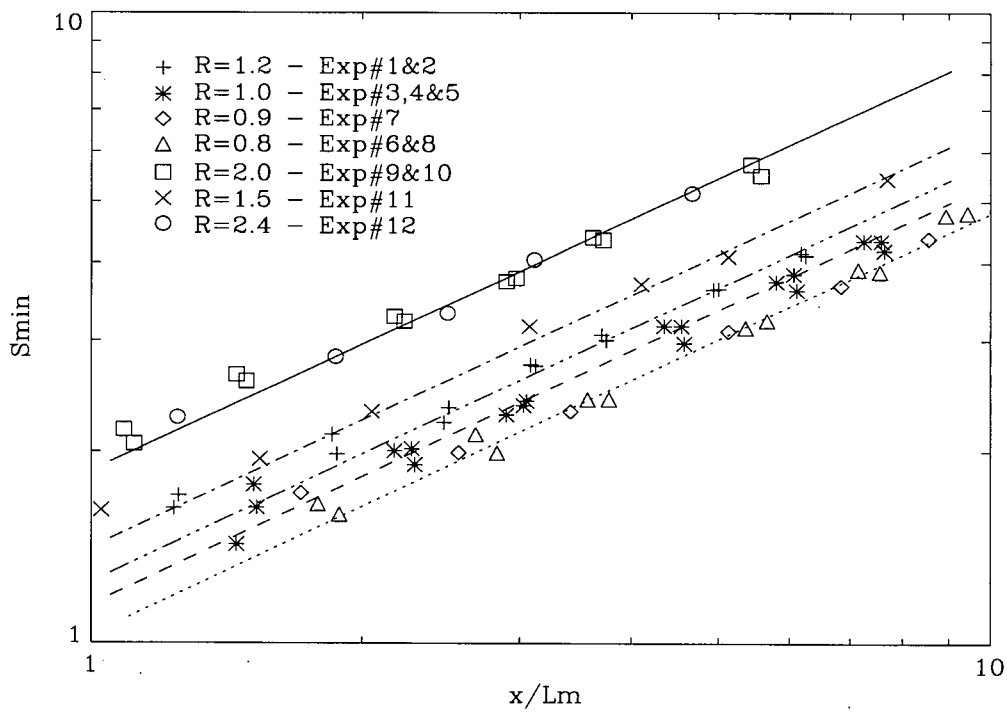

(b)

Figure 4. 2: (a) Plot of S_{min} versus x/L_m for the limits of velocity ratio, showing data points within the MDFF length scale range, $x>L_m$ and $x<L_M$, correlate to the 2/3 power. (b) Similar plot for all experiments showing that dilution is dependent on R.

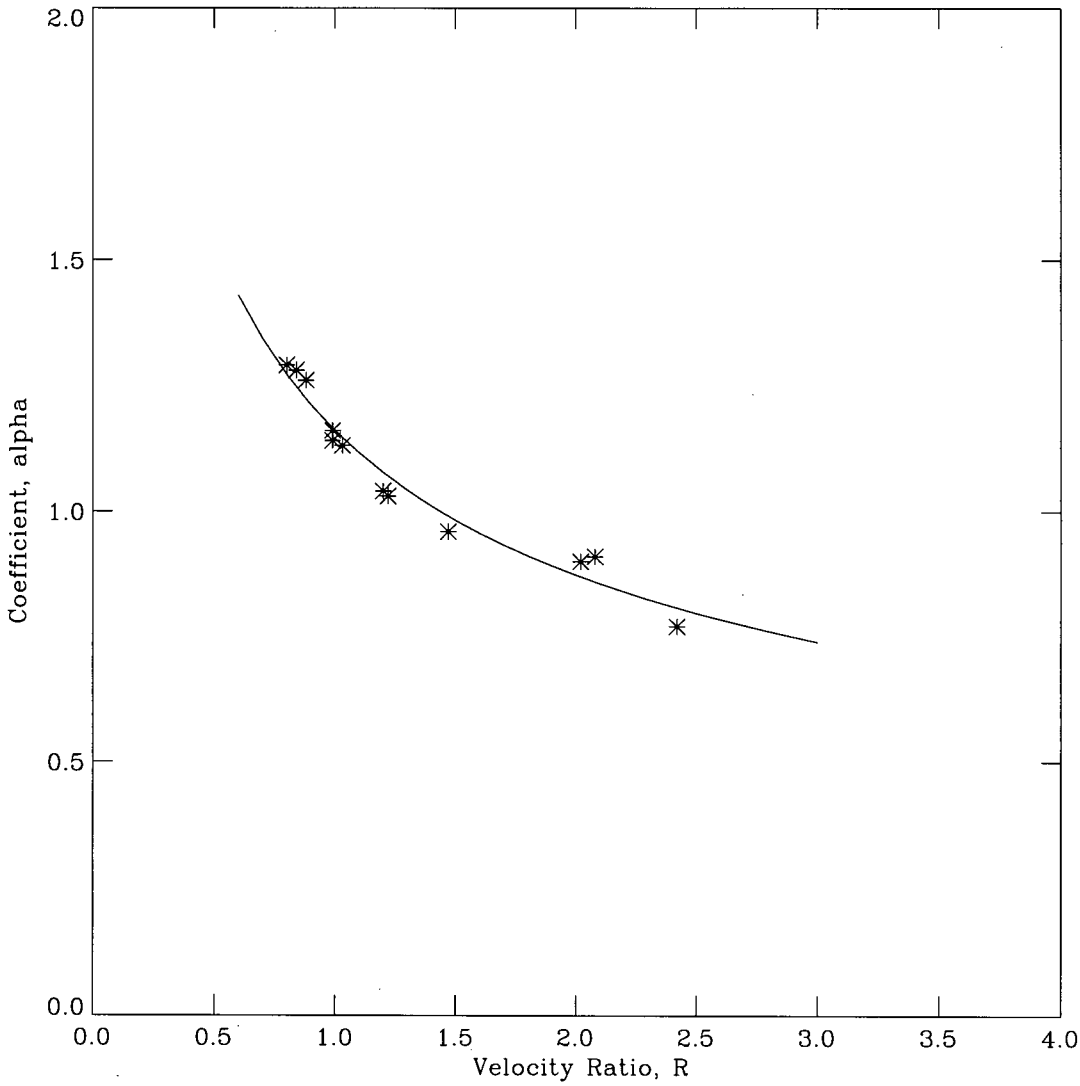

Figure 4. 3: Variation of experimental coefficient, α, with velocity ratio, R. The coefficient increases with decreasing R.

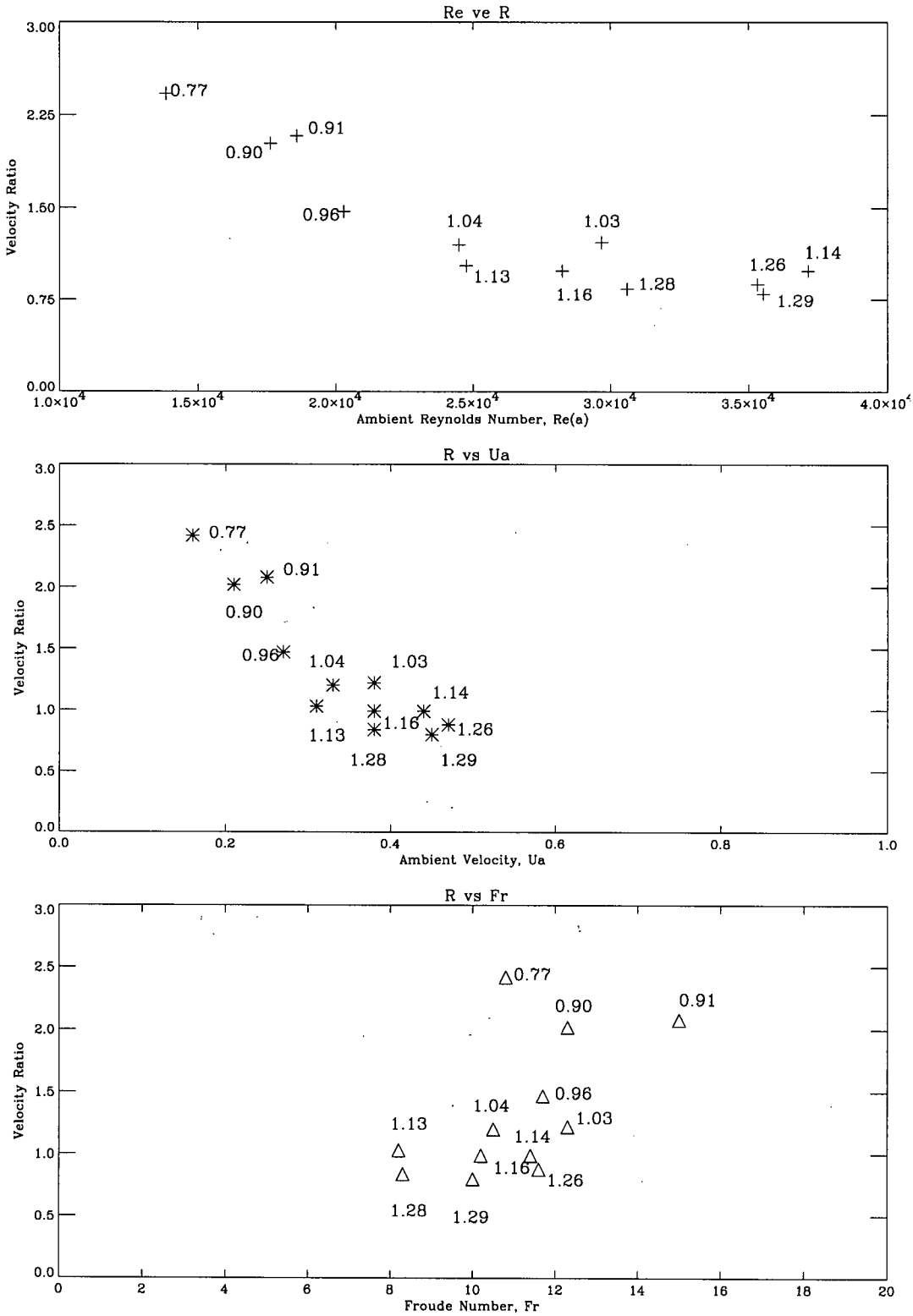

Figure 4. 4: Plots of velocity ratio versus changes in ambient Reynolds number, ambient velocity and jet Froude number along with respective coefficient α value.

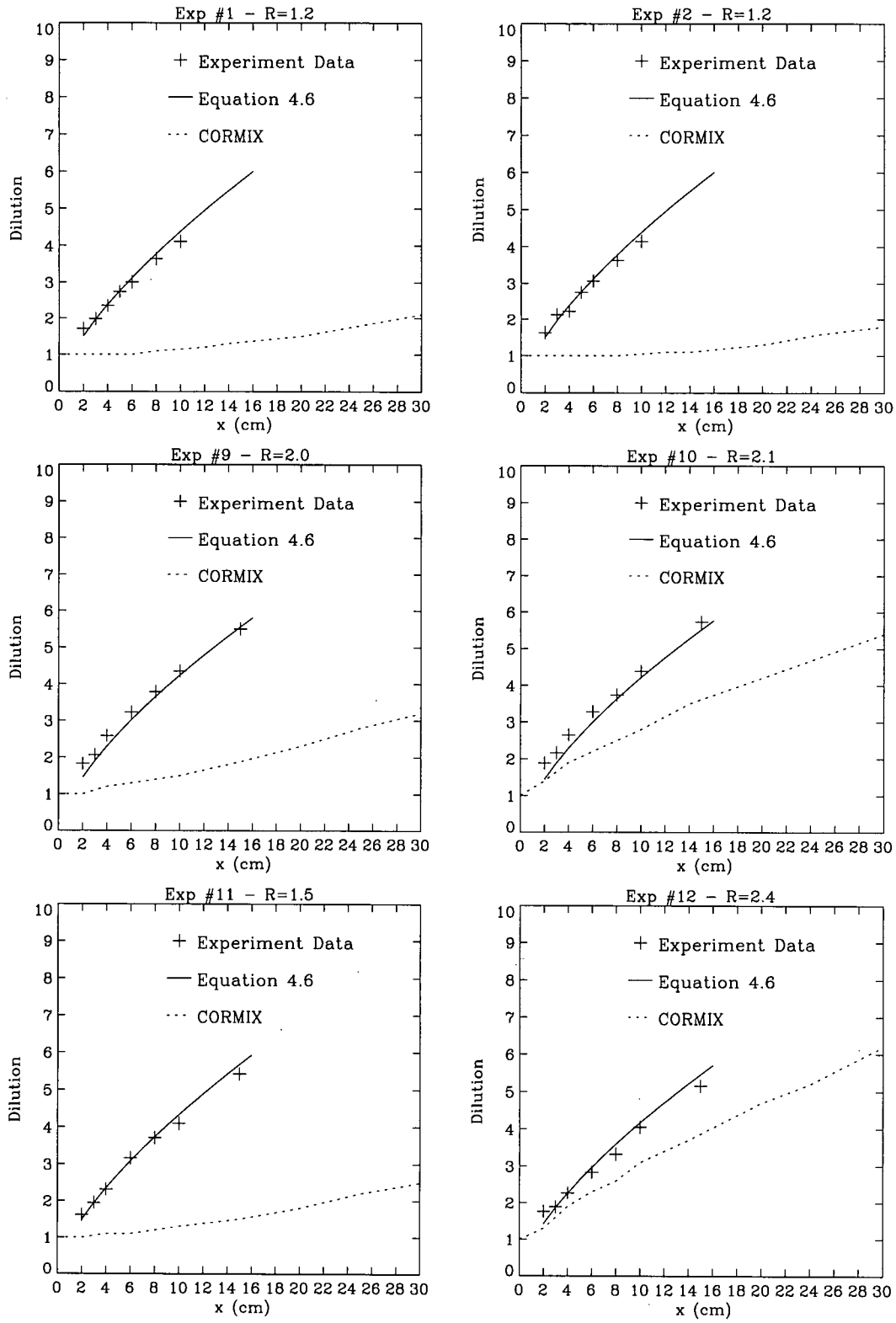

Figure 4. 5: Comparison of experimental dilution data with CORMIX 1 output for R > 1.

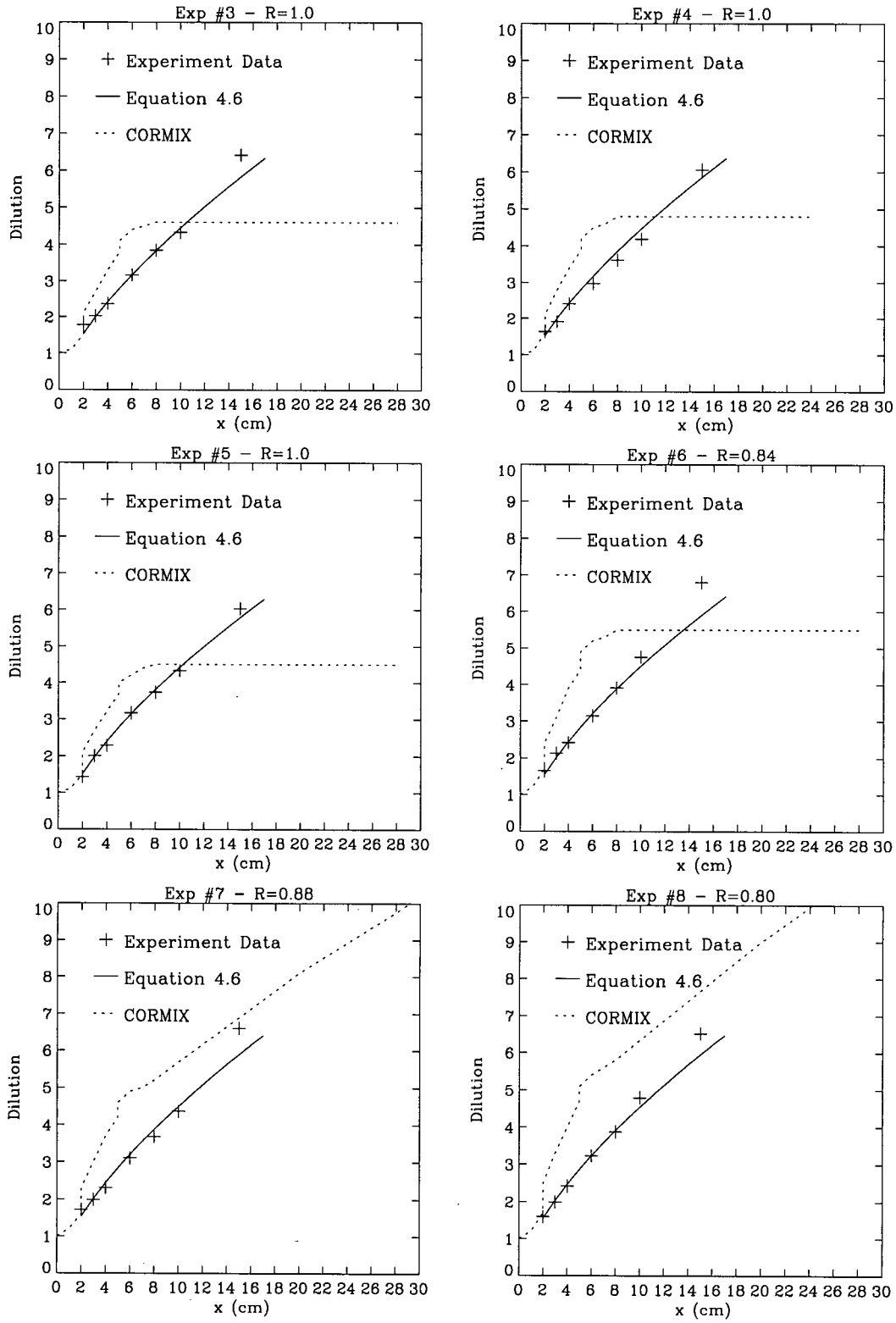

Figure 4. 6: Comparison of experimental dilution data with CORMIX 1 output for R ≤ 1.

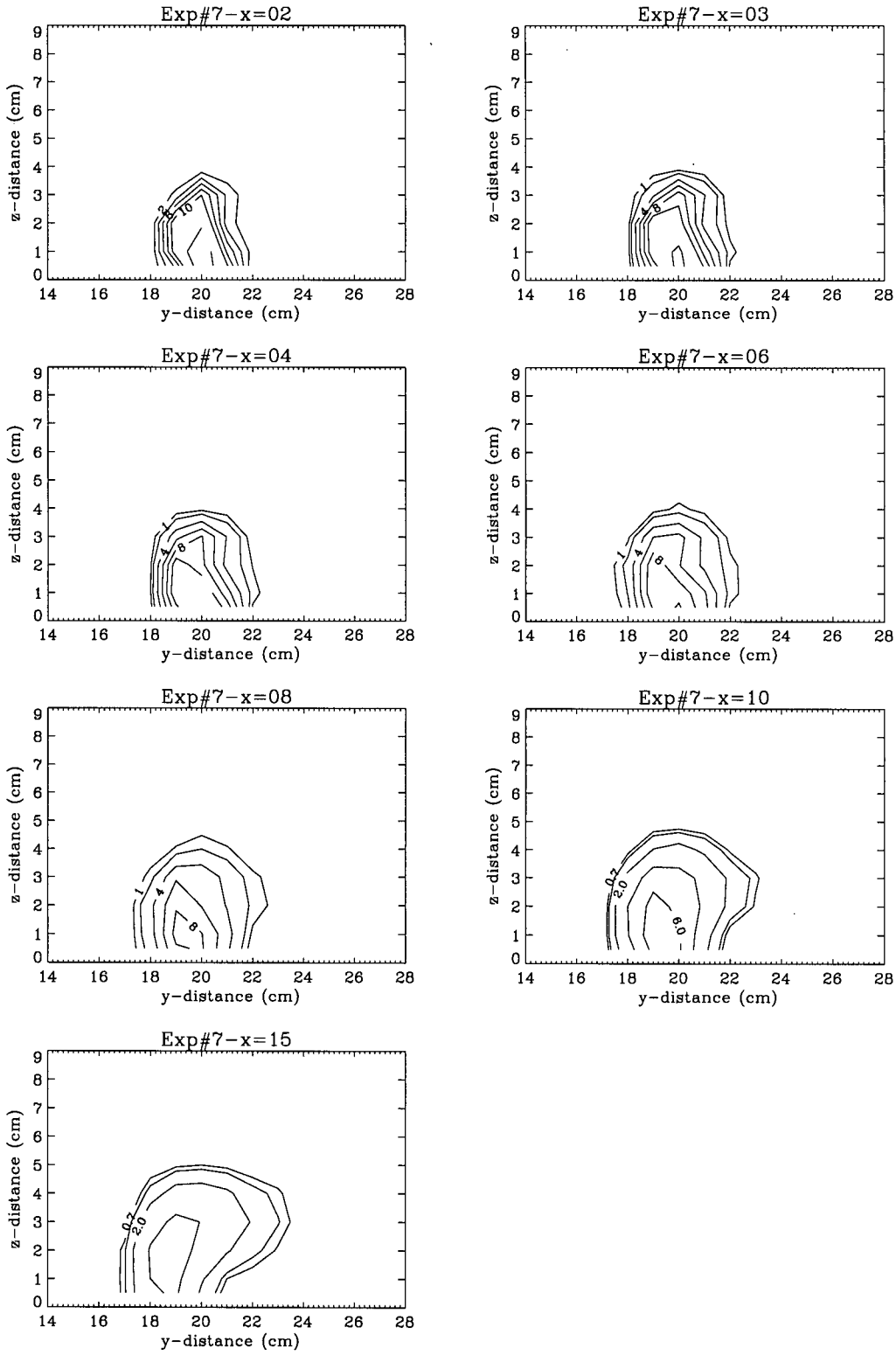

Figure 4. 7: Contour plot of excess temperature, defined as the temperature above ambient, for experiment #7. Each frame shows the jet at a farther downstream station.

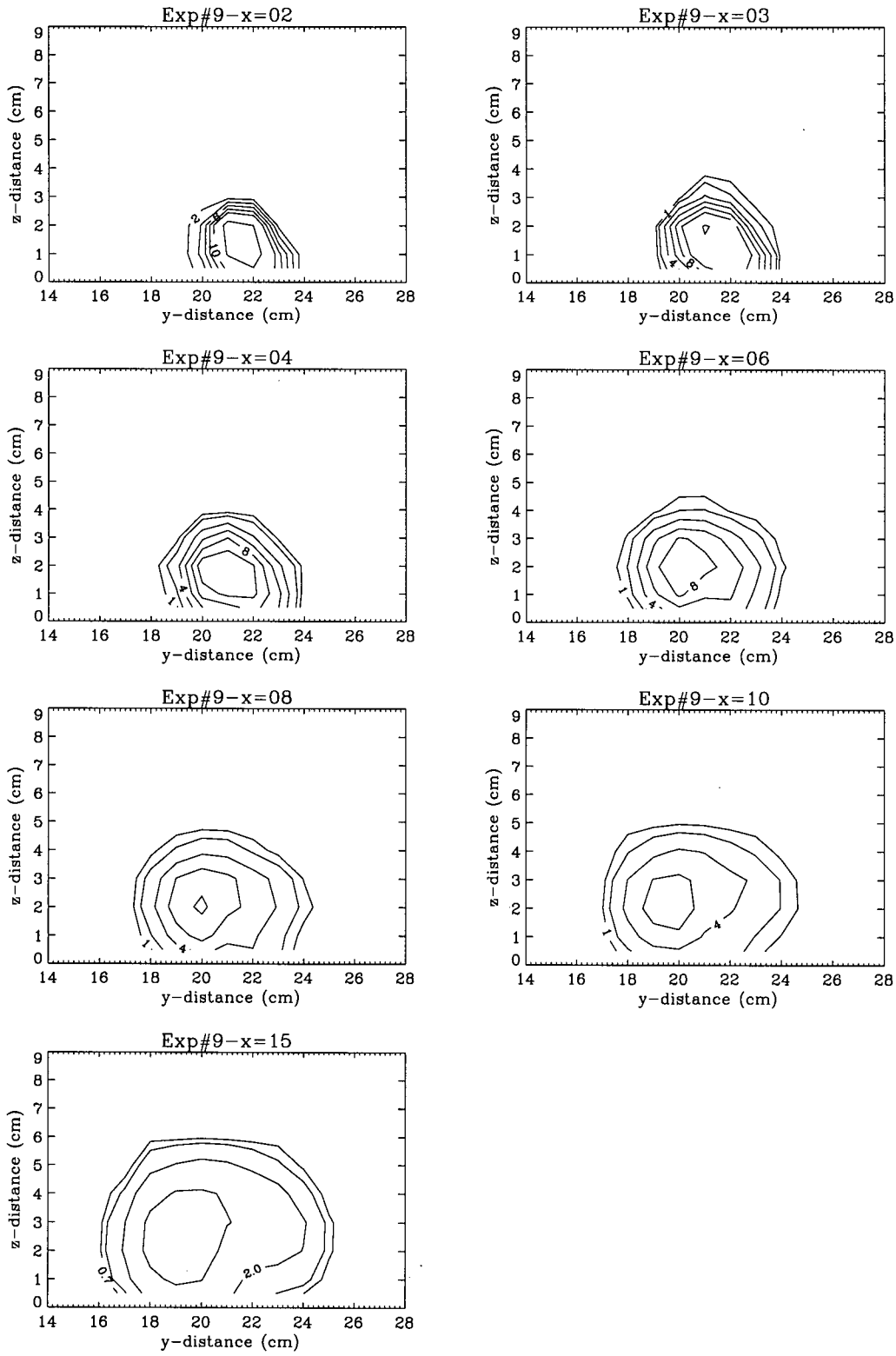

Figure 4. 8: Contour plots of excess temperature, defined as the temperature above ambient, for experiment #9. Each frame shows the jet at a farther downstream location.

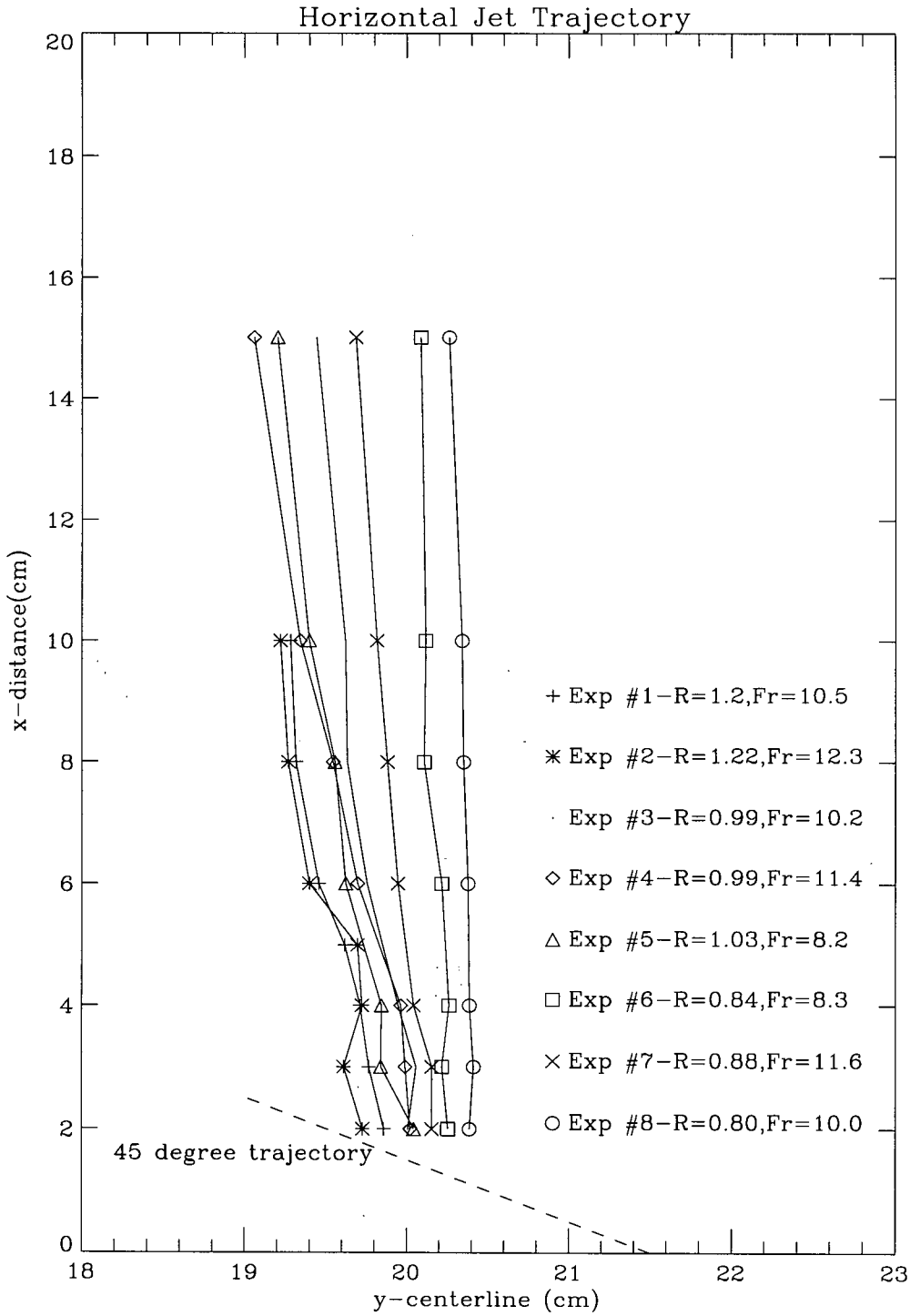

Figure 4. 9: Jet trajectory in the y-x plane for experiments 1 to 8. Jet is quickly advected by the ambient current and the penetration distance reduces with decreasing R.

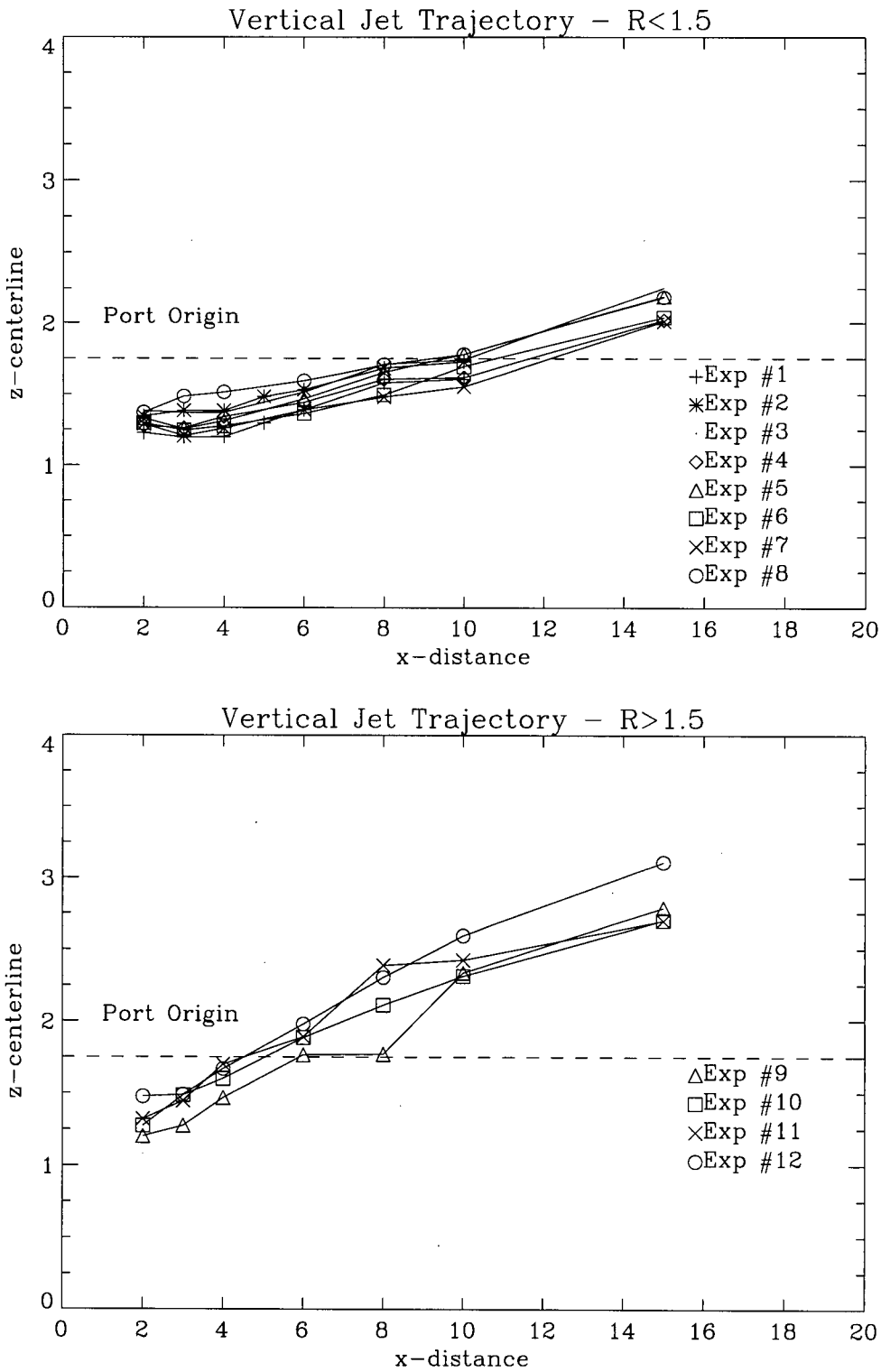

Figure 4. 10: Jet trajectory in the x-z plane for experiments 1 to 8 and experiments 9 to 12. Jet centerline is attracted towards the bed due to possible Coanda attachment of jet.

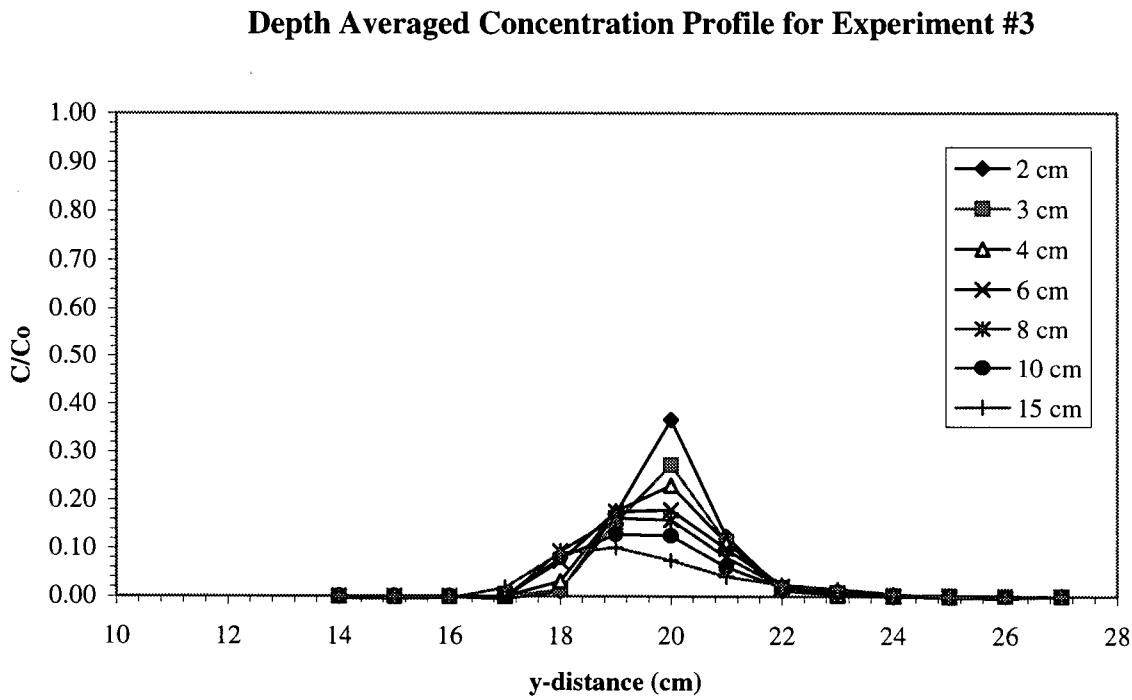

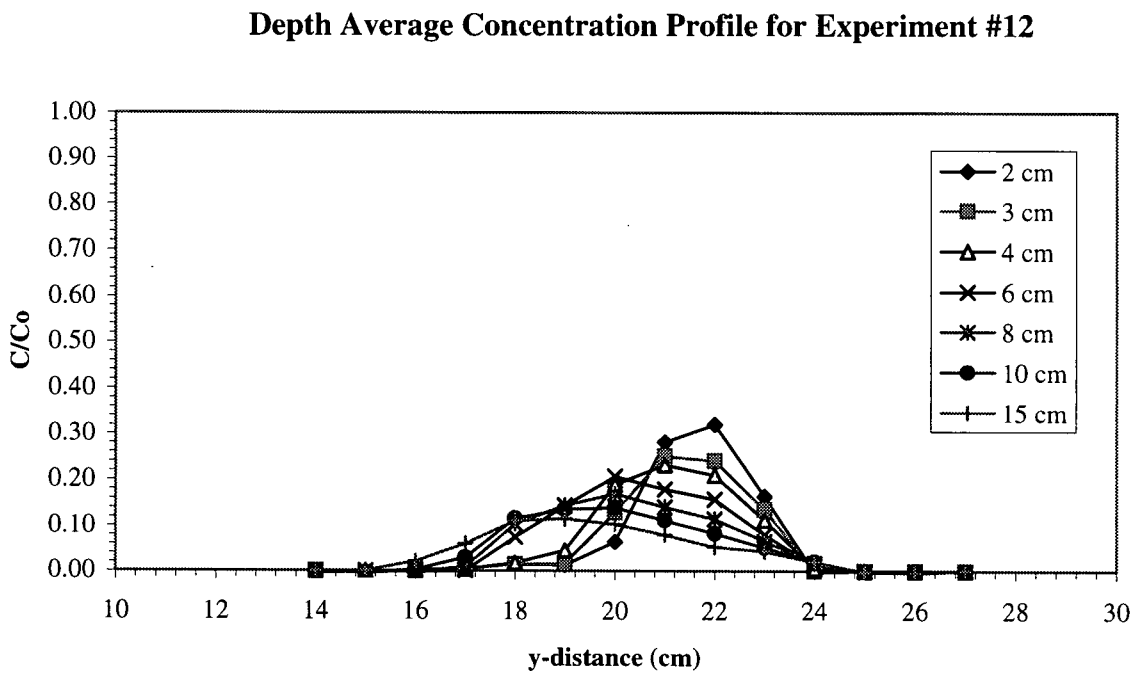

Figure 4. 11: Depth average horizontal concentration profiles for experiments #3 and 12. The jet horizontal width increases with distance and decreasing ambient velocity.

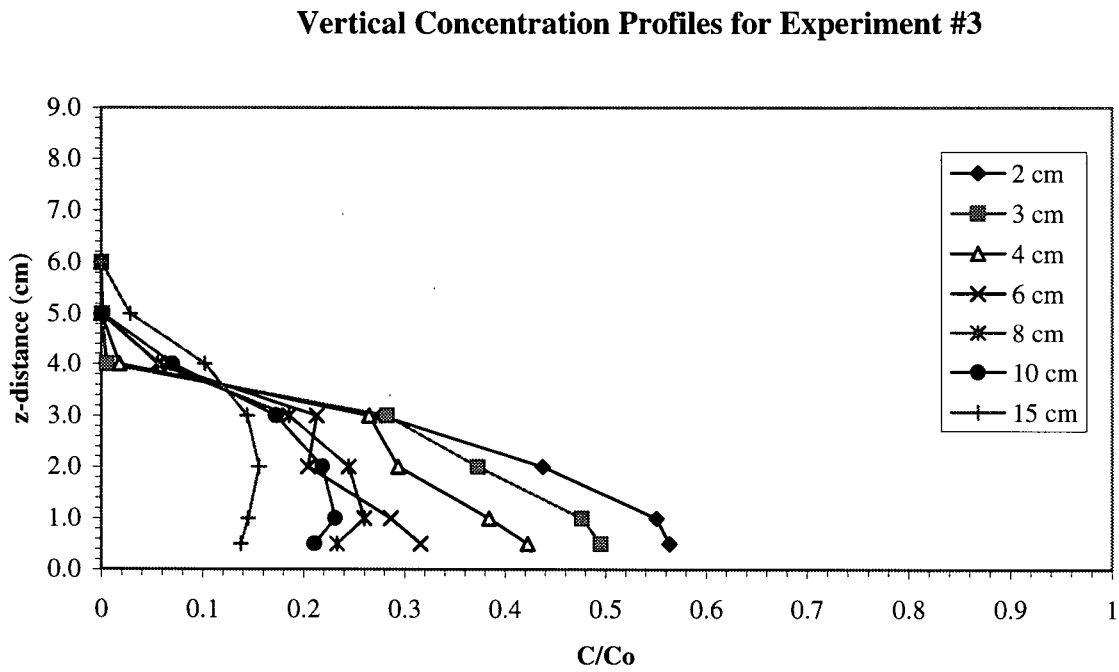

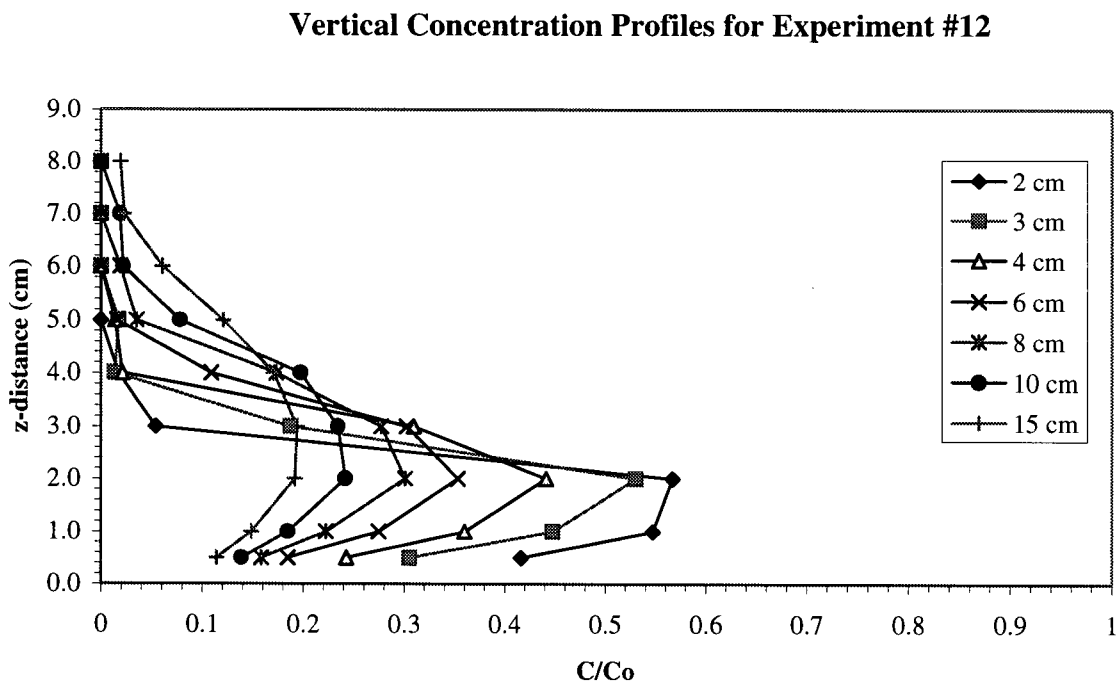

Figure 4. 12: Vertical concentration profiles with distance for experiments #3 and 12. Profiles show vertical jet width increases with distance and decreasing ambient velocity. Higher velocities promote attachment of the jet to the flume bottom.

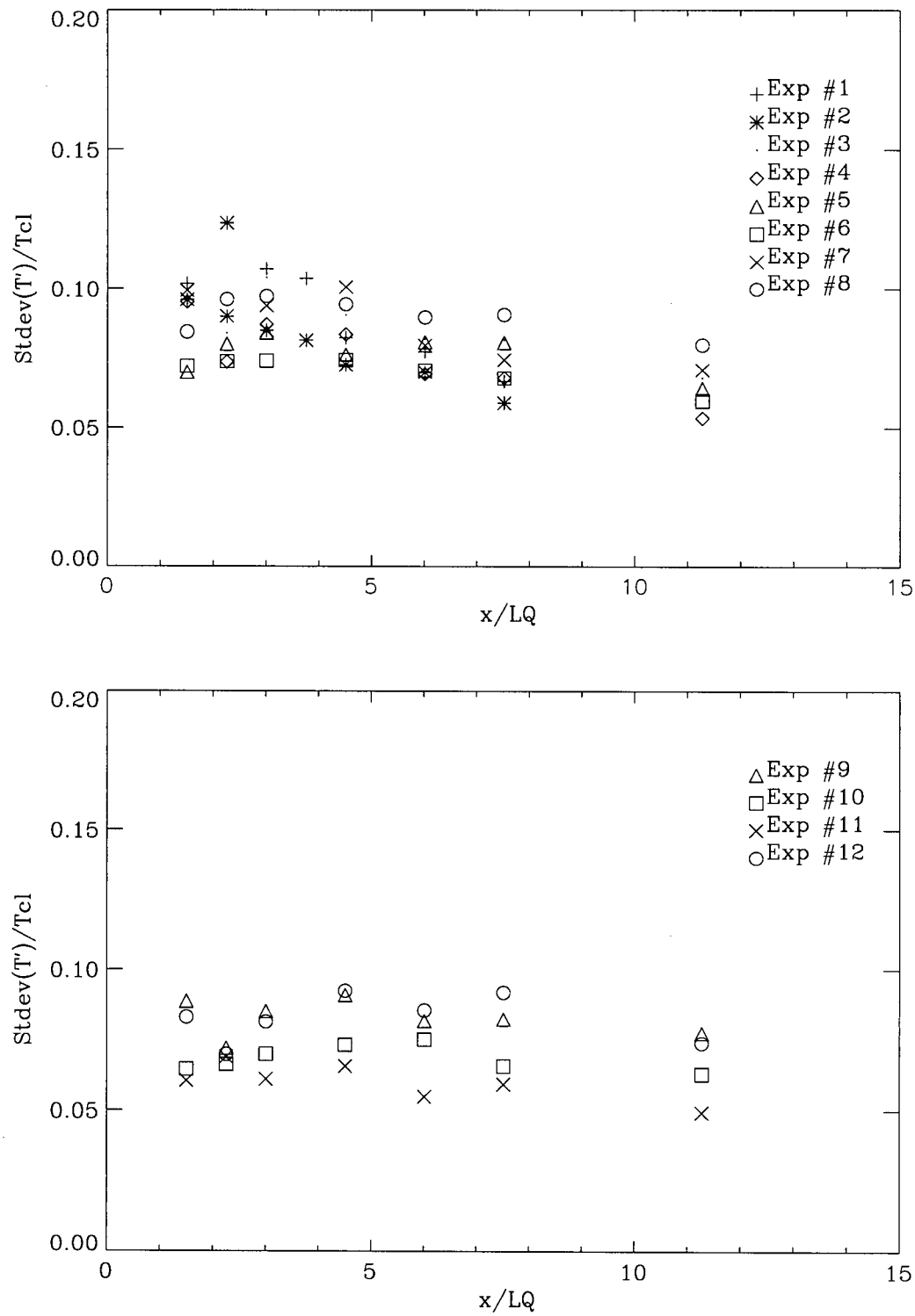

Figure 4. 13: Plot of maximum turbulence intensity with distance away from source. Turbulence intensity is on order of 0.1.

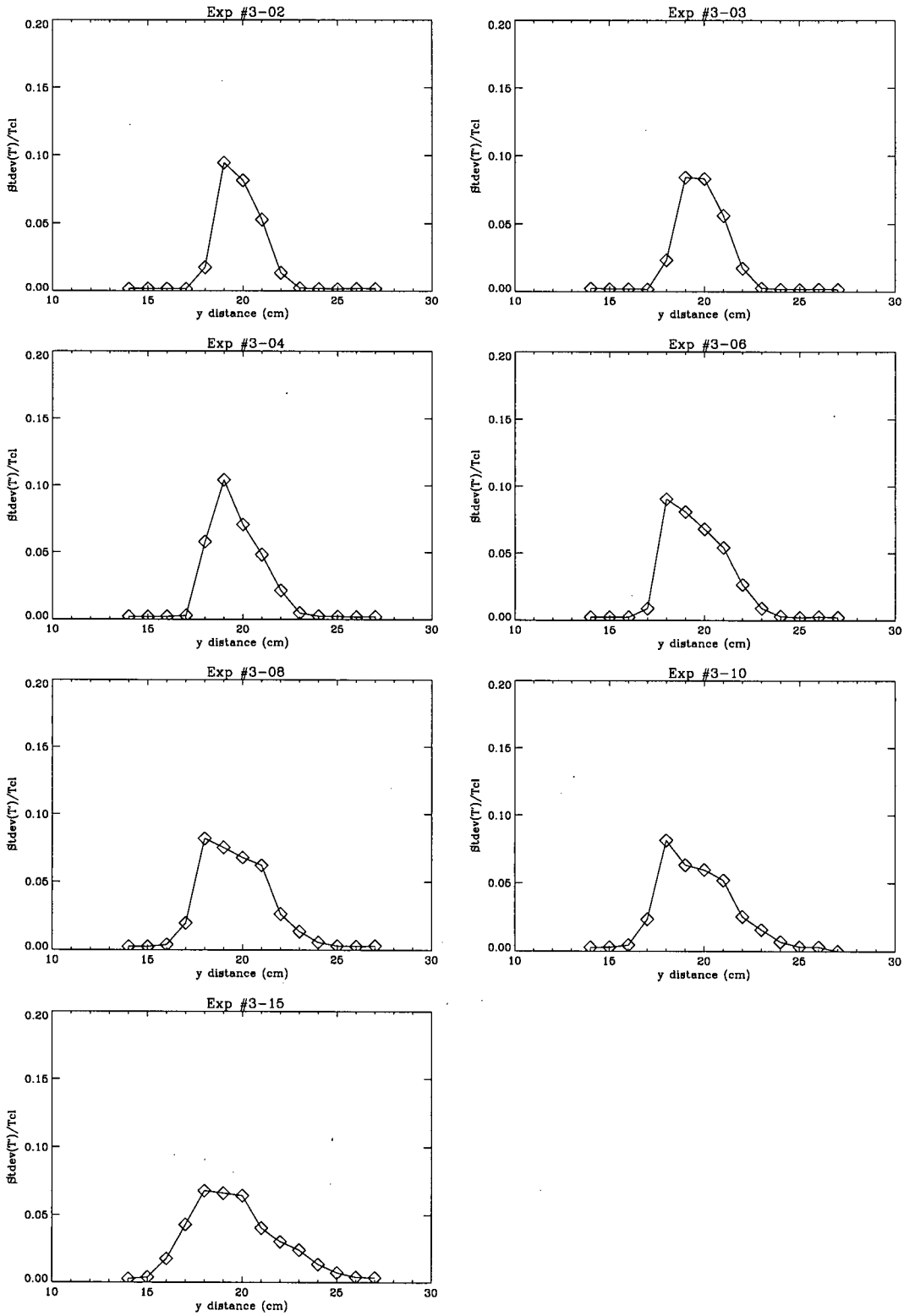

Figure 4. 14: Depth averaged horizontal turbulence intensity profiles for experiment #3. The width of the turbulent zone increases and peak values decrease with distance.

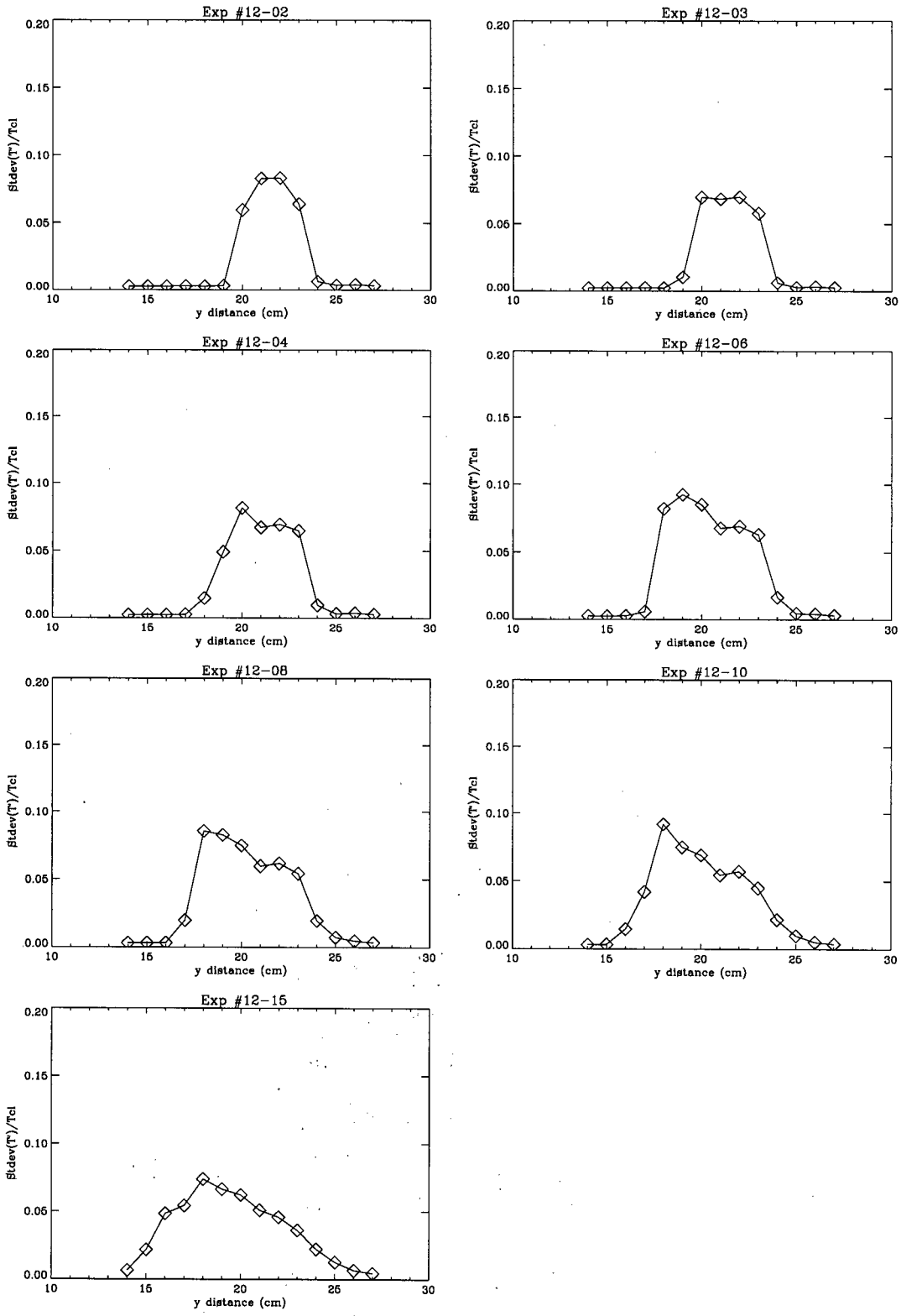

Figure 4. 15: Depth averaged horizontal turbulence intensity profiles for experiment #12. Peak values are slightly higher on the side where the current initially impacts the jet.

5.0 CONCLUSIONS AND RECOMMENDATIONS

This chapter will summarize the results of the study discussed in chapter four, highlight the main conclusions, discuss the relevance of the study to the Fraser River and present recommendations for further research.

5.1 Summary of Experiment Results

In the experiments performed, the velocity ratio has a greater influence than the densimetric jet Froude number on dilution. For the range of Froude numbers, 8 to 15, examined, there is no effect on the initial dilution. Dilution is shown to increase with decreasing velocity ratio. In the region investigated, jet momentum and ambient current play a more dominant role in mixing than the buoyancy factor. This is confirmed by the calculation of length scales which indicate momentum-dominated far-field flow behaviour for all experiments.

The velocity ratio and ambient current are the governing parameters for the case of a weak jet discharging into a strong current. Higher ambient velocities restrict plume growth in the vertical and horizontal directions as shown by the temperature contour plots and the concentration profiles. The trajectory calculations show that the jet is quickly deflected by the strong current and penetrates farther into the ambient water with higher velocity ratios. The vertical trajectories of the experiments show a tendency of the jet centerline to be initially attracted towards the flume bottom. When the ambient current is smaller, the length of attraction is shortened and the jet is quicker to mix vertically. The vertical concentration profiles show that the jet is more likely to attach to the flume bottom when the ambient velocity is larger than the jet velocity.

The data shows that using temperature to calculate dilution is reasonable. A temperature-time series is a good way to delineate a turbulent jet and turbulence intensities can be calculated from the series. In the experiments, the calculated turbulence intensities are greater where the current impacts the jet, resulting in greater temperature fluctuations. Turbulence intensities are on order of 0.1 and slightly higher for experiments involving a weak jet in a strong current.

5.2 Main Conclusions

The experimental data supports that length scales are a good indication of flow behaviour even for discharge angles other than 90 degrees and strong ambient currents. For the experiments performed, the calculated length scales indicate that the jet should resemble a momentum dominated, strongly deflected jet in the area examined. The dilution data supports this jet type by corresponding well with the momentum dominated far-field dilution relationship developed from previous research, that is,

$$\frac{S}{R} = \alpha\left(\frac{x}{L_m}\right)^{2/3} \tag{5.1}$$

The 2/3 power dependence held for the data even though the angle was 45 degrees, the port was close to bed and the presence of a strong ambient current. However, the coefficient α was found to be higher than previous research and vary exponentially with the velocity ratio, R. The coefficient increases with lower velocity ratios. The best fit line is

$$\alpha = 1.16R^{-0.41} \tag{5.2}$$

No definite conclusions can be drawn from the study to explain why α is dependent on the velocity ratio. However, α is probably a function of many parameter such as the angle of discharge, port diameter, proximity to bed, water depth, jet Froude number and ambient turbulence levels.

5.3 Applicability to Northwood and the Fraser River

Some remarks can be made in relation to the interaction between the Northwood effluent discharge and the Fraser River.

1) The individual jets on the Northwood multiport diffuser act as weak, momentum-dominated jets in a strong current as shown by the dilution data corresponding to the MDFF relationship, calculated length scales and CORMIX 1 computer model. Therefore in the initial dilution zone, the buoyancy force due to the density difference between the effluent and river water is expected to have minimal influence on mixing.

2) Dilution calculations confirm that buoyancy does not affect the initial dilution and therefore, seasonal changes in temperature are unimportant in the initial zone. However, seasonal changes in ambient velocity will have a great influence on dilution and the entrainment process. Dilution would be the highest during the spring freshet when the ambient velocity and turbulence levels increase.

3) Turbulence intensity data shows that the interaction between the effluent plume and river would be turbulent and therefore, the area in the vicinity of the port has the potential to be an important area of interaction between sediment and effluent biosolids with the velocity ratio being a controlling mechanism.

4) There is an indication that the jet attaches to bottom which is of importance to the Fraser River since this will affect benthic communities in the near-field. Also, there is the possibility of entrainment and transport of deposited sediment from this mechanism.

The conclusions drawn from the experimental data are applicable to the Northwood and Fraser River site since the range of Froude numbers and velocity ratios examined are the same. There is no dependence on the Reynolds number because in both cases the jet and ambient flows are turbulent. Therefore, the model results with regards to dilution as a function of distance can be applied to the actual case by using the length scale ratio of prototype to model which is 33 and a third.

5.4 Recommendations

Further research in this area is recommended to better understand the mixing process in the near-field zone.

1) Examination of the buoyancy dominated region, the area beyond the MDFF were the jet is changing to a plume before it surfaces, would be of interest.

2) Further experimental work of benefit would be flow visualization and velocity measurements for a single port discharging at a range of horizontal angles.

3) Collection of field data on the initial dilution in the vicinity of Northwood diffuser is recommended for comparison with experimental work.

6.0 REFERENCES

Chu, V.H. (1985). Oblique Turbulent Jets in a Crossflow. Journal of Engineering Mechanics, 111 (11), 1343-1359.

Evans, W. (1996). Flocculation of Fraser River Sediments Due to Pulp Mill Effluents. Draft M.A.Sc. thesis, University of British Columbia, Vancouver.

Fischer, H.B., List, E.J., Koh, R.C., Imberger, J., and Brooks, N.H. (1979). Mixing in Inland and Coastal Waters. London, Academic Press.

Gaskin, S.J. (1995). Single Buoyant Jets in a Crossflow and the Advected Line Thermal. Ph.D. thesis, University of Canterbury.

Gobas, F.A.P.C. (1996). Modelling the Fate of Contaminant Discharges in the Fraser River Basin. In Proceedings of the 3rd DOE Research Workshop. Vancouver.

Jirka, G.H. and Fong, H.L. (1981). Vortex Dynamics and Bifurcation of Buoyant Jets in Crossflow. Journal of Engineering Mechanics, 107 (EM3), 479-497.

Jirka, G.H. and Doneker, R.L. (1991). Hydrodynamic Classification of Submerged Single-Port Discharges. Journal of Hydraulic Engineering, 117 (9), 1095-1112.

Johnston, A.J., Nguyen, N. and Volker, R.E. (1993). Round Buoyant Jet Entering Shallow Water in Motion. Journal of Hydraulic Engineering, 119 (12), 1364-1382.

Johnston, A.J., Phillips, C.R. and Volker, R.E. (1994). Modelling Horizontal Round Buoyant Jet in Shallow Water. Journal of Hydraulic Engineering, 120 (1), 41-59.

Johnston, A.J., Nguyen, N. and Volker, R.E. (1994). Round Buoyant Jet Entering Shallow Water - Bed Shear. Journal of Hydraulic Research, 32 (2), 233-250.

Knudsen, M. (1988). Buoyant Horizontal Jets in an Ambient Flow. Research Report 88-7, University of Canterbury, New Zealand.

Krishnappen, B.G., Stephens, R., Kraft, J.A. and Moore, B.H. (1994). Size Distribution of Suspended Particles in the Athabasca River near Hilton. National Water Research Institute, Canadian Centre for Inland Waters.

Lee, J.H. and Jirka, G.H. (1981). Vertical Round Buoyant Jet in Shallow Water. Journal of the Hydraulics Division, ASCE, 107, 1651-1675.

Lee, J.H. and Neville-Jones, P. (1987). Initial Dilution of a Horizontal Jet in Crossflow. Journal of Hydraulic Engineering, 113 (5), 615-629.

Lee, J.H. (1989). Notes on Ayoub's Data of Horizontal Round Buoyant Jet in Current. Journal of Hydraulic Engineering, 115 (7), 969-975.

Marmorek, D.R., Korman, J., Bernard, D.P. and Berry, T. (1992). Ecosystem Fate and Effects of Pulp Mill Effluents in the Fraser River: Identification of research and monitoring priorities. Prepared by ESSA Ltd., Vancouver, B.C. for Inland Waters Directorate, Environment Canada, North Vancouver.

Papanicola, P.N. and List, E.J. (1988). Investigations of Round Vertical Turbulent Buoyant Jet. Journal of Fluid Mechanics, 195, 341-391.

Rajaratnam, N. and Langat, J.K. (1995). Mixing Region of Circular Turbulent Wall Jets in Crossflows. Journal of Hydraulic Engineering, 121 (10), 694-698.

Sekela, M., Brewer, R., Baldazzi, C. and Moyle, G. (1995). Change in Contaminant Concentration in Fraser River Suspended Sediments and Water During the Onset of Freshet (Marguerite - 1993) (DRAFT REPORT). North Vancouver: Aquatic Section, Science Division, Environmental Conservation Branch, Pacific and Yukon Region, Environment Canada.

Sekela, M., Brewer, R., Baldazzi, C., Moyle, G., and Tuominen, T. (1995). Survey of Contaminants in Suspended Sediment and Water in the Fraser River Basin. Report DOE FRAP 1995-21, Environmental Conservation Branch, Pacific and Yukon Region, Environment Canada, Vancouver.

Sobey, R.J, Johnston, A.J. and Keane, R.D. (1988). Horizontal Round Buoyant Jet in Shallow Water. Journal of Hydraulic Engineering, 114 (8), 910-929

Tsanis, I.K. and Valeo, C. (1994). Mixing Zone Models for Submerged Discharges. Environmental Hydraulics Vol 1, Computational Mechanics Publications.

Vine, J. (1996). Random Walk Models Applicable to Rivers. Draft M.A.Sc. thesis, University of British Columbia, Vancouver.

Wong, C.F. (1991). Advected Line Thermals and Puffs. M. Phil, University of Hong Kong, Hong Kong.

Wood, I.R., Bell, R.G. and Wilkinson, D.L. (1993). Ocean Disposal of Wastewater. World Scientific.

Wright, S.J. (1977). Mean Behavior of Buoyant Jets in a Crossflow. Journal of Hydraulic Engineering, 103 (HY5), 499-513.

APPENDIX A: Thermocouple Calibration Information

A thermocouple is an electrical circuit consisting of two dissimilar metals joined at each end to make a circuit, through which an electromagnetic force is developed. They allow for temperature measurements over a wide range and at a small point. T-type thermocouples, made of copper and Constantan, were used in the experiments.

Calibrations curves (Figure A.1) were developed for all 16 thermocouples which involved submerging the thermocouples in their experimental configuration into a water bath of known temperature. The water bath temperature was measured using a mercury thermometer. The voltage produced by each thermocouple for a certain temperature was recorded as given by the data acquisition program. The temperature range was approximately 5 to 50 degrees Celsius which is representative of the temperature range that the thermocouples would experience during the experiments. Linear regression was performed on each data set to calculate a slope and offset for the 16 thermocouples (Table A.1). This data was used as an input file for the computer program developed by Scott Jackson of UBC to turn voltage readings into temperature measurements.

Table A. 1: Calibration Slope and Offset Values for Individual Thermocouples

Thermocouple #	Slope	Offset
T1	25.6114	-0.7463
T2	25.6853	-0.747
T3	25.7162	-0.7496
T4	25.6678	-0.7485
T5	25.4021	-0.765
T6	25.3726	-0.7632
T7	25.3575	-0.7592
T8	25.3256	-0.756
T9	25.4499	-0.7392
T10	25.3414	-0.7484
T11	25.3973	-0.746
T12	25.4115	-0.7462
T13	25.3059	-0.7514
T14	25.3626	-0.7467
T15	25.4011	-0.7428
T16	25.3582	-0.7646

Temperature = slope*voltage + offset

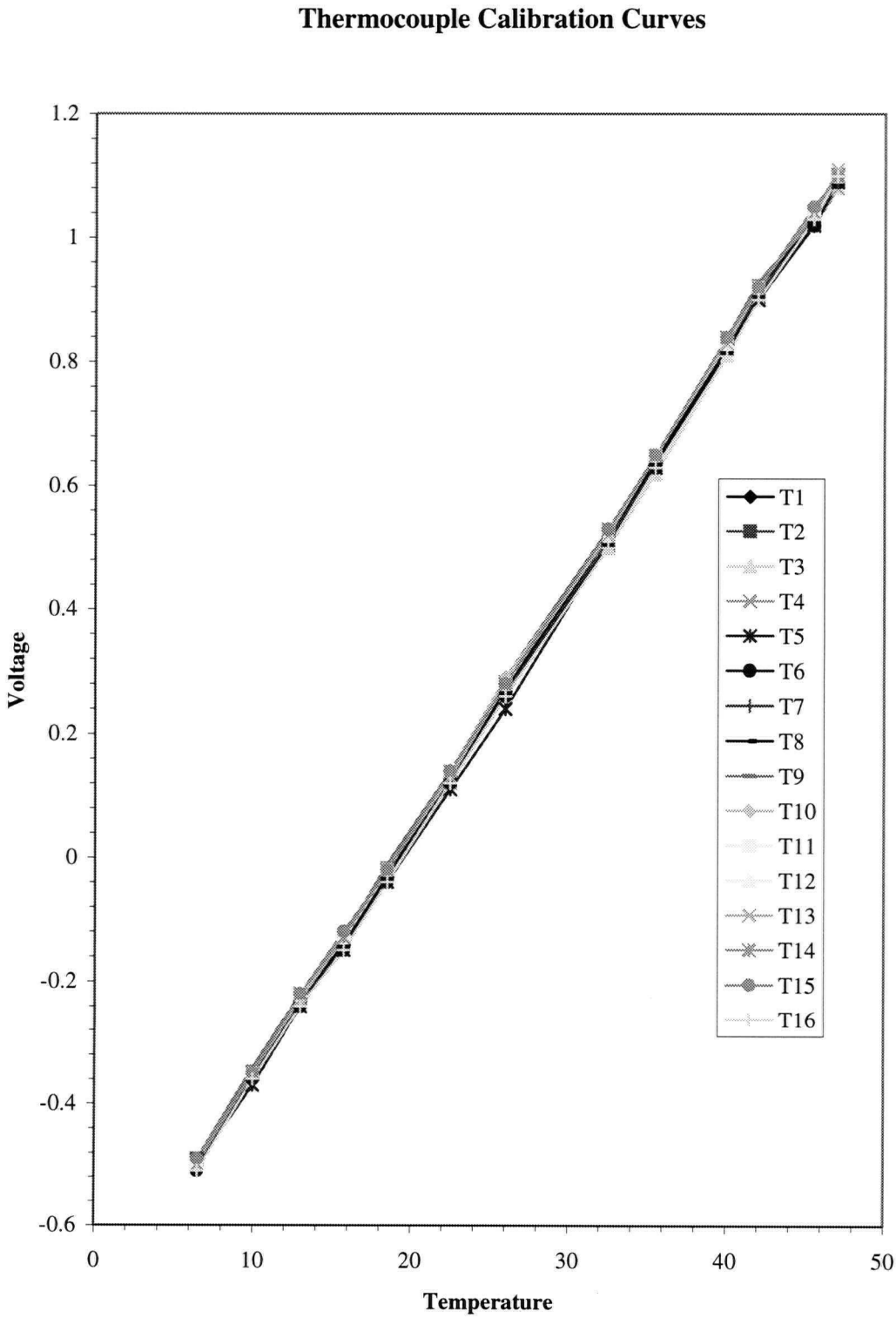

Figure A. 1: Calibration curves for individual thermocouples